Journal of Marine Systems 111–112 (2013) 139–156

Contents lists available at SciVerse ScienceDirect

Journal of Marine Systems

journal homepage: www.elsevier.com/locate/jmarsys

The rise and fall of the "marine heat wave" off Western Australia during the summer of 2010/2011

Alan F. Pearce [a,b,*], Ming Feng [c]

[a] Western Australian Department of Fisheries, P.O. Box 20, North Beach, WA 6920, Australia
[b] Curtin University, GPO Box U1987, Perth, WA 6845, Australia
[c] CSIRO Marine and Atmospheric Research, Private Bag 5, Wembley, WA 6913, Australia

ARTICLE INFO

Article history:
Received 24 April 2012
Received in revised form 24 August 2012
Accepted 11 October 2012
Available online 22 October 2012

Keywords:
Temperature
Continental shelves
Water currents
Mortality
Geographical distribution
Leeuwin Current
La Niña

ABSTRACT

Record high ocean temperatures were experienced along the Western Australian coast during the austral summer of 2010/2011. Satellite-derived sea surface temperature (SST) anomalies in February 2011 peaked at 3 °C above the long-term monthly means over a wide area from Ningaloo (22°S) to Cape Leeuwin (34°S) along the coast and out to >200 km offshore. Hourly temperature measurements at a number of mooring sites along the coast revealed that the temperature anomalies were mostly trapped in the surface mixed layer, with peak nearshore temperatures rising to ~5 °C above average in the central west coastal region over a week encompassing the end of February and early March, resulting in some devastating fish kills as well as temporary southward range extensions of tropical fish species and megafauna such as whale sharks and manta rays. The elevated temperatures were a result of a combination of a record strength Leeuwin Current, a near-record La Niña event, and anomalously high air–sea heat flux into the ocean even though the SST was high. This heat wave was an unprecedented thermal event in Western Australian waters, superimposed on an underlying long-term temperature rise.

1. Introduction

The "marine heat wave" which was experienced off Western Australia in the austral summer of 2010/2011 had some remarkable (and in a few cases, devastating) consequences for the marine biota along the continental shelf (Smale and Wernberg, 2012; Thomson et al., 2011; Wernberg et al., 2012). In early 2011, fish kills were reported along many sections of the Western Australian coastline, and some iconic species such as whale sharks and manta rays were encountered much further south than their normal latitudinal ranges (Pearce et al., 2011). As will be shown, water temperatures rose rapidly above the long-term monthly means as this thermal event unfolded, peaking at the end of February/early March along most of the coastline. The anomalously warm conditions were associated with one of the strongest La Niña events on record (as indicated by the Southern Oscillation Index and the Multivariate ENSO Index: Wolter and Timlin, 1998; see also Beard et al., 2011; Bureau of Meteorology, 2012) and a near-record strength Leeuwin Current.

Ocean temperatures off Western Australia are some 5 °C higher than at equivalent latitudes in other eastern boundary current (EBC) regions in the Southern Hemisphere because of the poleward-flowing Leeuwin Current, which brings warm, low-salinity tropical waters southwards and then eastwards along the south coast of the continent (Cresswell and Golding, 1980; Pearce, 1991). In the "traditional" EBCs, cool equatorward current systems are associated with seasonally-varying wind-driven upwelling events and result in some of the richest scale-fisheries in the world. By contrast, the dominant fisheries in the nutrient-poor oligotrophic waters off Western Australia are benthic invertebrates, especially the western rock lobster *Panulirus cygnus* (Lenanton et al., 1991).

The Leeuwin Current is relatively shallow (~300 m deep) and narrow (~100 km wide) and normally flows most strongly during the austral autumn to early spring months (April–October) (Feng et al., 2003; Godfrey and Ridgway, 1985; Smith et al., 1991; Woo and Pattiaratchi, 2008). Monthly mean ocean temperatures off Perth (Fig. 1) in summer and winter are approximately 22.3° and 19.2 °C respectively, whereas the seasonal water temperature ranges at the same latitude along the west coasts of South Africa (the Benguela Current) and South America (the Humboldt Current) are 18.4°–14.5 °C and 17.0°–13.0 °C respectively (Pearce, 1991).

The southward flow and relatively warm oceanic regime off Western Australia have resulted in a "marine-overlap" zone between tropical and temperate species along the coast of Western Australia (Wilson and Allen, 1987) as well as the transport of tropical marine fauna down the west coast and around into the Great Australian Bight (Maxwell and Cresswell, 1981).

* Corresponding author at: Western Australian Department of Fisheries, P.O. Box 20, North Beach, WA 6920, Australia. Tel.: +61 8 9203 0111; fax: +61 8 9203 0199.
E-mail addresses: alanpearce@iinet.net.au (A.F. Pearce), ming.feng@csiro.au (M. Feng).

0924-7963/$ – see front matter © 2012 Elsevier B.V. All rights reserved.
http://dx.doi.org/10.1016/j.jmarsys.2012.10.009

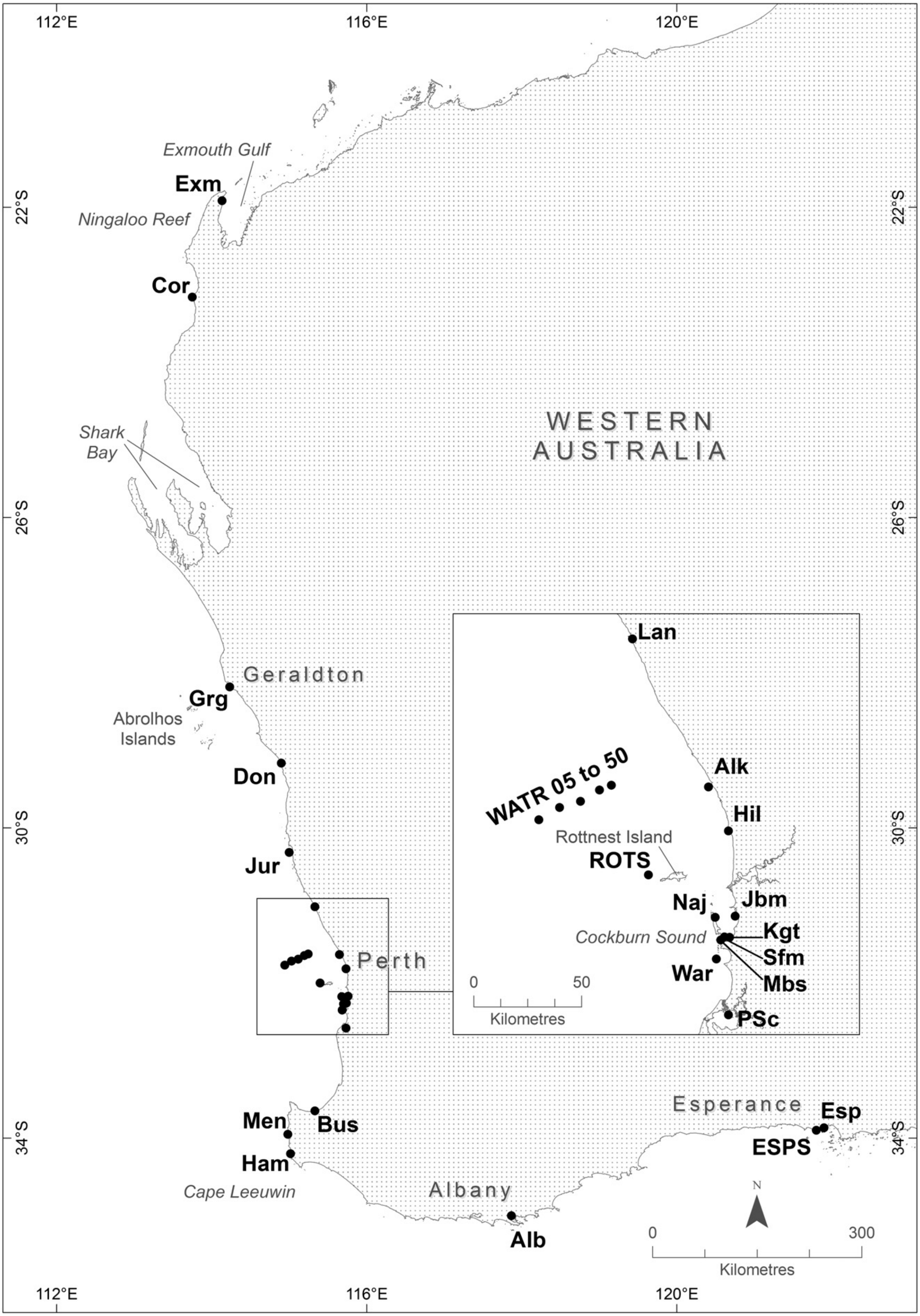
112°E
116°E
120°E
22°S
26°S
30°S
34°S
Exmouth Gulf
Exm
Ningaloo Reef
Cor
WESTERN
AUSTRALIA
Shark
Bay
Geraldton
Grg
Abrolhos
Islands
Don
Jur
Perth
Lan
Alk
WATR 05 to 50
Hil
Rottnest Island
ROTS
Naj
Jbm
Cockburn Sound
Kgt
Sfm
War
Mbs
0
50
Kilometres
PSc
Esperance
Esp
ESPS
Men
Bus
Ham
Cape Leeuwin
Albany
Alb
N
0
300
Kilometres

Water temperatures off Western Australia also vary interannually, largely associated with the El Niño/Southern Oscillation (ENSO) cycle. During La Niña periods, relatively high coastal sea levels are indicative of a strongly-flowing Leeuwin Current which transports more warm water southwards (Feng et al., 2003, 2008; Pearce and Phillips, 1988) while during El Niño events the Leeuwin Current is weaker and the water temperature generally (but not universally) lower (Pearce et al., 2006). Monthly temperature anomalies in the Leeuwin Current region vary by up to ±1.5 °C in El Niño and La Niña periods. This interannual variability in the flow of the Leeuwin Current and the related water temperature both play a major role in recruitment and subsequent catches to many commercial fisheries (Caputi et al., 2010; Lenanton et al., 2009) — this is most evident for the rock lobster fishery where annual settlement of the puerulus stage during El Niño periods is appreciably lower than in La Niña years (Caputi et al., 2001; Clarke and Li, 2004; Lenanton et al., 1991; Pearce and Phillips, 1988).

Underlying these seasonal and interannual variations in the water temperature is a gradually-rising temperature trend which appears to be associated with global warming, and the waters immediately offshore of Western Australia are warming more rapidly than the average over the Indian Ocean (Caputi et al., 2009; Pearce and Feng, 2007).

Water temperature plays a major role in the growth and survival of most marine organisms, affecting all developmental stages of the life-cycle (Byrne, 2011) and accordingly tends to largely govern the distribution and abundance of many species. Generally, warmer water (within limits) leads to more rapid larval development and growth in both fish and invertebrates (Caputi et al., 2010; Chittleborough, 1975; Munday et al., 2007), but above a certain optimal temperature for each species, metabolic activity reduces (Sylvester, 1972). Both rapid short-term temperature rises and more prolonged exposure to consistently elevated temperatures can be harmful or even lethal to fish (e.g. Kim et al., 2001) — Hobbs and McDonald (2010) reported a mass mortality during abnormally elevated temperatures and calm water conditions at the Cocos Islands in the equatorial Indian Ocean during two warming events in 2007–2008 and April 2009, as the fish were exposed to temperatures (33° to 35 °C) above their thermal tolerance. Further, longer-term temperature trends such as those associated with climate change can push a species beyond its capacity to adapt and thus have a direct effect on the species distribution (Neuheimer et al., 2011). In the North Sea, for example, there has been a noted shift in the latitudinal distribution of a number of species, and as pointed out by Perry et al. (2005), such range extensions may have a significant impact on commercial fisheries.

Similar warming events have been experienced elsewhere in the world. In the northern summer of 2003, for example, the anomalous persistence of high atmospheric pressure associated with almost no wind and very high surface air temperature (Black et al., 2004) over the western continental Europe and the western Mediterranean basin, resulted in a significant heat wave event (e.g., Black et al., 2004; Schar et al., 2004). Sutton and Hodson (2004) attributed this and other extreme atmospheric events over Western Europe and eastern North America at the time to a multi-decadal climatic oscillation of Atlantic sea surface temperatures, known as the Atlantic Multidecadal Oscillation (AMO). A substantial increase in air temperature, a decrease in wind stress and reduction of all components of the upward heat flux resulted in heating of the sea surface by 3–4 °C (Olita et al., 2007; Sparnocchia et al., 2006), which was almost as severe as the heating off Western Australia in early 2011. This heat wave may have induced steep declines in shoot abundance of *Posidonia oceanica* meadows and therefore represented a significant threat to the important seagrasses in the Mediterranean (Marba and Duarte, 2010).

This paper describes the development, extent and decay of the warm water event off Western Australia during the austral summer of 2010/2011 using the available temperature measurements, and also summarises some of the biological consequences. Both large-scale (monthly) surface water temperatures and hourly measurements from in situ temperature loggers over the period of the heat wave are presented in Section 3 together with an assessment of the likely mechanisms contributing to the elevated temperatures (the potential roles of the Leeuwin Current, the ENSO cycle and air–sea heat flux). Section 4 documents some of the abnormal biological observations resulting from the warming event.

While this heat wave was a discrete (albeit extreme) environmental event, it is perhaps a warning of the potentially disastrous implications of any similar events which may occur in the future.

2. Data and methods

2.1. Large-scale SSTs

Large-scale sea surface temperatures (SSTs) for the south-eastern Indian Ocean have been obtained from the Reynolds SST analysis (Reynolds and Smith, 1994; website www.emc.ncep.noaa.gov, accessed August 2011) from January 1982. The temperatures are based on satellite thermal infrared measurements supplemented by in situ monitoring from drifting buoys and ships, providing monthly mean SSTs on 1-degree latitude/longitude blocks (100 km * 100 km). This scale encompasses the Leeuwin Current and offshore waters, but the shape of the coastline in relation to the latitude/longitude blocks means that some blocks are almost exclusively on the continental shelf whereas others extend across the shelf and Current. The long-term (1982 to 2010) mean seasonal cycle for each block has been derived and the anomalies from this cycle over the period of the heat wave have been calculated. In addition, the time-series of monthly SSTs and the anomalies in selected coastal blocks along the continental shelf between Exmouth and Esperance have been extracted.

2.2. Local temperatures

The development of the heat wave on the continental shelf and nearshore waters can be assessed from self-recording temperature loggers located at a number of monitoring sites along the Western Australian coast and offshore islands. These unpublished measurements were generously provided by government departments, research organisations, universities and commercial companies and covered different time periods although all were operational during at least the central part of the heat wave. The sites and sources for all the available logger records are listed with the main results in Table 1.

Most of the measurements were made using Onset Stowaway Tidbit loggers having a nominal accuracy of about 0.2 °C at the temperatures found off south-western Australia. Occasional calibration checks were undertaken of some loggers and these showed that they were normally accurate to within ±0.1 °C. Temperatures were sampled hourly at most sites, although 1/4 or 1/2 hourly measurements were made in some cases and these have been converted to hourly by averaging over 1/2-hour centred on the hour. Daily averages were derived and form the basis of this analysis to show the alongshore extent and temporal evolution of the heat wave. For those sites where at least 3 years of valid measurements were available, the anomalies of the daily temperatures from these "long-term" means (which varied between 3 and 10 years) for the month-long period 15th February to 15th March were calculated. Some of the anomalies differ slightly from those listed

Fig. 1. Chart showing the places mentioned in the text and the locations of the temperature loggers (filled circles — see Table 1 for the coded abbreviations). The inset shows more detail of the region off Perth; the 4 IMOS WATR Two Rocks stations are in depths of 200 m, 150 m, 100 m and 50 m. There is a group of sites in Cockburn Sound, and 4 sites are clustered around Rottnest Island. Because of congestion, not all the sites listed in Table 1 are actually named in this figure.

Table 1
Dates and peak daily temperatures from temperature loggers and other instruments during the marine heat wave of January–March 2011. Where there were 3 years or more or valid data from 2000 to 2010, the anomaly of the peak temperature above the long-term mean for February–March has been included. For the 3 south coast sites, column 2 contains the longitude.

Site (code)	Latitude (°S)	Date of peak temp. 2011	Peak temp (anomaly) (°C)	Source
Exmouth (Exm)	21° 55′	24-Jan	31.2°	Hoschke (Curtin)
Coral Bay (Cor)	23° 10′	24-Jan	29.6°	Rossbach (DoF)
Pt. Gregory (Grg)	28° 11′	28-Feb	28.9° (5.0°)	Rossbach (DoF)
Rat Island (Rat)	28° 42′	1-Mar	28.7° (5.0°)	Rossbach (DoF)
Rat Island (Ako2)	28° 44′	1-Mar	29.3°	Starling (FRDC)
Pelsaert Is. (Ako3)	28° 53′	1-Mar	28.4° (4.3°)	Starling (FRDC)
Dongara (Don)	29° 10′	26-Feb	29.4° (5.1°)	Rossbach (DoF)
Jurien (Jur)	30° 19′	27-Feb	28.3° (5.6°)	Rossbach (DoF)
Lancelin (Lan)	31° 01′	27-Feb	27.5° (4.4°)	Marrs (Murdoch)
Alkimos (Alk)	31° 38′	28-Feb	27.1° (3.8°)	Rossbach (DoF)
WATR05 (TR05)	31° 38′	6-Mar[a]	25.4°	IMOS mooring
WATR10 (TR10)	31° 39′	6-Mar[a]	25.6°	IMOS mooring
WATR15 (TR15)	31° 42′	27-Feb	26.6°	IMOS mooring
WATR20 (TR20)	31° 43′	28-Feb	27.0°	IMOS mooring
Hillarys (Hill)	31° 49′	28-Feb	26.5° (4.5°)	Rossbach (DoF)
Hillarys Marina (HilM)	31° 50′	28-Feb	26.9° (3.3°)	Seaframe (BoM)
CSIRO Station (ROTS)	32° 00′	26-Feb	25.1°	IMOS mooring
Rottnest (RotW1)	32° 01′	4-Mar	25.6°	Thomson (CSIRO)
Rottnest (RotS)	32° 01′	28-Feb	26.2°	Hoschke (Curtin)
Rottnest (RotPP1)	32° 01′	1-Mar	25.7°	Hoschke (Curtin)
Rottnest (RotPP2)	32° 01′	28-Feb	26.3°	Pearce (Curtin)
Rottnest (RotW2)	32° 02′	28-Feb	26.1°	Thomson (CSIRO)
Cockburn Snd (Naj)	32° 10′	1-Mar	26.2° (2.9°)	Marsh (DoF)
Cockburn Snd (Jbm)	32° 11′	27-Feb	27.0°	Marsh (DoF)
Cockburn Snd (Mbs)	32° 16′	28-Feb	26.4°	Marsh (DoF)
Cockburn Snd (Sfm)	32° 16′	1-Mar	26.1° (2.9°)	Marsh (DoF)
Cockburn Snd (Kgt)	32° 16′	2-Mar	25.8° (2.6°)	Marsh (DoF)
Warnbro Snd (War)	32° 21′	1-Mar	26.6° (3.4°)	Rossbach (DoF)
Peel Estuary (PSc)	32° 35′	26-Feb	28.8° (5.2°)	Marsh (DoF)
Busselton (Bus)	33° 39′	28-Feb	25.6° (3.7°)	Micha (BJECA)
Hamelin Bay (Ham)	34° 15′	5-Mar[a]	24.1° (3.2°)	Wernberg (UWA)
Albany (Alb)	~118°E	11-Mar	23.2°	Moyes (Dept. Transp)
Esperance (Esp)	~122°E	27-Feb	22.3° (1.9°)	Seaframe (BoM)
Esperance Stn. (ESPS)	~122°E	22-Mar	20.8°	Seaframe (BoM)

[a] Denotes that at these sites, there were also secondary peaks on 26th to 28th February, in line with the dates of the other peak temperatures. Some of the anomalies differ slightly from those in Pearce et al. (2011) as they were derived in a different way (see text).

in Pearce et al. (2011) as the means were derived from 3 or more years instead of the 5 or more years used by Pearce et al. (2011).

The northernmost logger was at the Piercam facility run by Curtin University on the navy pier near Northwest Cape (Exmouth Gulf — Fig. 1 and Table 1). The Coral Bay, Port Gregory, Rat Island, Dongara, Jurien, Alkimos, Hillarys and Warnbro Sound loggers were at the near-shore (~5 m depth) Department of Fisheries puerulus collection sites (Cor, Grg, Rat, Don, Jur, Alk, Hil and War in Fig. 1 and Table 1), some of which have data going back for almost a decade (with some gaps). The Lancelin logger (Lan) is part of a Murdoch University study around Lancelin Island, while the University of Western Australia operated a logger on the seabed in about 10 m water depth in Hamelin Bay (Ham) near Cape Leeuwin (Smale and Wernberg 2009). A number of temperature loggers were deployed in the waters around Rottnest Island (Table 1 and Fig. 1) by CSIRO and Curtin University.

A comprehensive series of temperature measurements has been made at 8 sites in the Houtman Abrolhos Islands since September 2007 (Cropp et al., 2011), and 2 sites have been selected for the present analysis, representing Rat Island (Ako2) and Pelsaert Island (Ako3). As part of an invertebrate monitoring programme in Cockburn Sound (Fig. 1) and the Peel–Harvey system, 5 loggers have been operating in the Sound and 2 in the P–H estuary, only one of which (PSc) is available for analysis here — these are valuable as they are in partially enclosed water bodies and are therefore to some extent insulated from direct exchange with the open shelf waters. A logger has been operating at the end of the 1.4 km long Busselton Jetty (Bus) in about 10 m water depth since 2002; this is the longest unbroken hourly temperature logger deployment off south-western Australia.

A CSIRO coastal monitoring station has been operating at a site in nominally 55 m water depth some 6 km west of Rottnest Island since 1950 (with gaps), with weekly to monthly surveys of vertical profiles of water temperature, salinity and nutrients using classical reversing thermometers. These temperatures were used in a study of the longer-term temperature rise along the Western Australian continental shelf (Caputi et al., 2009; Pearce and Feng, 2007). While the profiling surveys have become somewhat intermittent in recent years, a National Reference Station (NRS) with water quality measurements (code ROTS) was installed in November 2008 as part of the Integrated Marine Observing System (IMOS) Australian National Mooring Network (ANMN), with Sea-Bird Electronics SBE39 temperature recorders at nominal depths of 30 m and 37 m in 50 m water depth. These instruments have a specified accuracy of ± 0.002 °C. The sampling interval was 5 min, and hourly values have been derived here by averaging the 7 readings between 1/4 before and 1/4 past the hour (e.g. 09:45 to 10:15). A similar NRS instrumented mooring (ESPS) was installed off Esperance on the south coast, commencing in November 2008, with temperature recorders at 30 m and 38 m depths in nominally 50 m water depth.

Hourly temperatures have also been obtained from the Seaframe monitoring stations operated by the Australian Bureau of Meteorology in Hillarys Marina (HilM) and at the Esperance Jetty (Esp; Fig. 1) since the early 1990s (with some gaps), and the Western Australian Department of Transport provided temperature data from a wave rider buoy off Albany (Alb) — the specifications of these instruments is not known, but the results would not be appreciably affected by small calibration differences.

2.3. Depth profiles

To assess the depth to which the warm water layer extended, temperature time-series have been obtained from the IMOS shelf moorings deployed off Two Rocks. The measurements commenced in July 2009 at mooring sites across the continental shelf and upper slope (Fig. 1), using Sea-Bird Electronics SBE39 temperature recorders. The moorings were in water depths of nominally 50 m (site WATR05, with 5 recorders between 25 and 46 m), 100 m (WATR10, 8 recorders between 25 and 96 m), 150 m (WATR15, 9 recorders between 25 and 146 m) and the 200 m isobath (WATR20, with 8 recorders between 30 m and 180 m depth); the actual instrument depths may have been somewhat different. The sampling interval was 10 min, and hourly values have been derived here by averaging the 3 readings over the hour (e.g. 09:50, 10:00 and 10:10).

Expendable BathyThermograph (XBT) temperature profiles have been obtained from the Royal Australian Navy for the outer shelf and upper slope off Perth for the period 16th to 23rd March — while this did not cover the peak of the heat wave, the mixed layer temperatures were nevertheless relatively high and the profiles provided information on the depth of the warm upper layer.

2.4. Meteorology and currents

Monthly values of the Southern Oscillation Index (SOI) were obtained from the Bureau of Meteorology (website http://www.bom.gov.au/climate/current/soihtm1.shtml accessed August 2011) and monthly Fremantle sea levels (FMSL — an index of the strength of the Leeuwin Current: Feng et al., 2003; Pearce and Phillips, 1988) were obtained from the University of Hawaii Sea Level Center (website ftp://ilikai.soest.hawaii.edu/woce/m175.dat accessed August 2011) for the period 1980 to 2011 to examine the relationships between the water temperatures, the Leeuwin Current and the ENSO cycle. The monthly sea levels were linearly detrended to remove the gradual rise in sea level over the past century, and the monthly anomalies were determined by subtracting the long-term annual cycle. To reduce small-scale variability and show the dominant patterns more clearly, a 3-month moving average filter was applied to the SOI and the sea level anomalies.

Because there were reports of unusually calm seas in some areas during the heat wave, hourly winds and air temperatures have been obtained from the Bureau of Meteorology Automatic Weather Station (AWS) sites located at North Island in the Abrolhos group (Fig. 1) and Rottnest Island. The former had sample rates of quasi-hourly and the latter 1-minute; in both cases, hourly time-series were derived for 2010–2011. In addition, monthly-averaged wave heights and periods for 2004 to 2011 were provided by the Western Australian Department of Transport for a wave-rider location near Rottnest Island.

Altimeter-derived surface current patterns were obtained from CSIRO (website http://www.cmar.csiro.au/remotesensing/oceancurrents/SW/ accessed October 2011) to show the mesoscale features of the Leeuwin Current, including the meander/eddy structure, over the peak heat wave period.

Monthly and daily values of the net air–sea heat flux were obtained from the European Centre for Medium-Range Weather Forecasts (ECMWF) ERA interim re-analysis (Dee et al., 2011) between 2006 and 2011, averaged over the region 22° to 33°S, 110°E to the coast (http://www.ecmwf.int/products/data/archive/descriptions/ei/index.html).

3. Physical characterization and mechanisms of the heat wave

The evolution and characteristics of the heat wave are described here using both the larger-scale (~100 km; Reynolds SST analysis) and local temperature measurements along the coast in 2010–2011, with a brief assessment of the main contributors to the warming event (Sections 3.4 and 3.5).

3.1. Large-scale development of the heat wave

The overall evolution of the heat wave can be followed using the monthly Reynolds SST anomaly charts for the period October 2010 to May 2011 (Fig. 2). The SST anomalies in October 2010 lay well within the normal historical range of ±1.5 °C. By November, however, a patch of water >2 °C above the long-term average appeared northwest of Exmouth Gulf, and this patch drifted south-eastwards to reach the Exmouth coast during December, before expanding both southwards and offshore in January and February 2011 as the water warmed even further. In January, the temperature anomaly exceeded 3 °C in a localised area just south of Exmouth, and over the following month a large area from north of Shark Bay to the Abrolhos Islands and out to >200 km offshore was affected; the >2 °C water extended from Exmouth to Geographe Bay and to over 500 km offshore, covering an area of some 600,000 km^2. By March, the >3 °C water had dissipated and the >2 °C patch had shifted southward to penetrate around Cape Leeuwin, beginning to cool and break up and by May the heat wave had effectively ended. It is interesting that as the heat wave was developing, the water in the far north was cooling across a wide area (see the January 2011 chart), and this progressively extended southwards across the North West Shelf and down to the latitude of Shark Bay.

The regional evolution of the heat wave can be examined more quantitatively using the monthly Reynolds SSTs and anomalies for selected coastal blocks from January 2010 to July 2011 (Fig. 3a). These show the expected latitudinal cooling trend down the west coast (Exmouth to Busselton) and across the south coast to Esperance. The 2010 seasonal cycle showed the peak temperature occurring in March along the west coast and in February on the south coast, with the trough consistently in September. During spring, the temperature rose steadily and by February 2011 the summer peak temperatures along the west coast were appreciably higher (and earlier) than in 2010; there was minimal heat wave signal at Albany and Esperance, most noticeably as an extension of the summer temperature into the autumn season.

Decoupling the seasonal pattern by deriving the monthly anomalies (Fig. 3b) clarifies the magnitude and phase shift of the peak temperatures with latitude. Following temperature anomalies within ±1 °C for most of 2010, as well as the dominantly negative temperature anomalies off the upper west coast during the first half of 2010 (likely a result of the 2009/2010 El Niño event), the water began to warm from October and climbed steadily into summer. There was a rapid phase transition from the "warm pool" El Niño to La Niña conditions in 2010, probably due to the Indian Ocean warming (Kim et al., 2011). The peak anomaly at Ningaloo was 3 °C in January, and there were even higher peaks between Shark Bay and the Abrolhos Islands in February. Down at Cape Leeuwin, the peak temperature was about 2.5 °C and occurred in March. These elevated temperatures gradually decayed to more typical levels between April and July.

3.2. Birth, growth, duration, decay of the heat wave on the continental shelf

While Figs. 2 and 3 illustrate the gross characteristics of the heat wave on the monthly scale, details of its evolution can be unravelled from the daily temperatures at the selected temperature logger sites along the coast. As shown in Table 1, the dates of the highest daily temperatures south of Coral Bay dominantly occurred over the week spanning the end of February and early March.

The alongshore (latitudinal) changes in daily temperature can be approximately divided into 3 regional groups delineated by the thick lines in Fig. 4: Exmouth and Coral Bay (the northern west coast), Port Gregory to Busselton (the mid- and lower west coast region), and Hamelin Bay to Esperance (the south coast). Up at Exmouth, the temperature rose gradually from about 24 °C in early October 2010 following the normal spring–summer transition, reaching a peak of over 31 °C on day 24 (24th January) — a rise of 7 °C over the 3–4 month period. The temperature then slowly declined through

February, March and April. Further south at Coral Bay (2nd curve in Fig. 4), the temperatures were almost universally lower and much more variable than at Exmouth, with some rises and falls of over 2 °C within 2 or 3 days during January but these were largely in phase with corresponding (albeit smaller) fluctuations at Exmouth as well as at some sites further south.

At the group of stations between Port Gregory and Busselton (a distance of almost 600 km), the heat wave appears to have occurred in two phases (Fig. 4). There was an initial and well-defined sharp temperature rise at most sites around day 355 in late December, the most dramatic of which was a 4 °C jump at Dongara over just 4 days (Fig. 4). This was followed by a plateau (incorporating smaller rises and falls in temperature) until mid February when a more general warming commenced, culminating in a week-long peak period during which the highest temperatures occurred — between days 57 (26th February) and 60 (1st March) at most sites. The highest

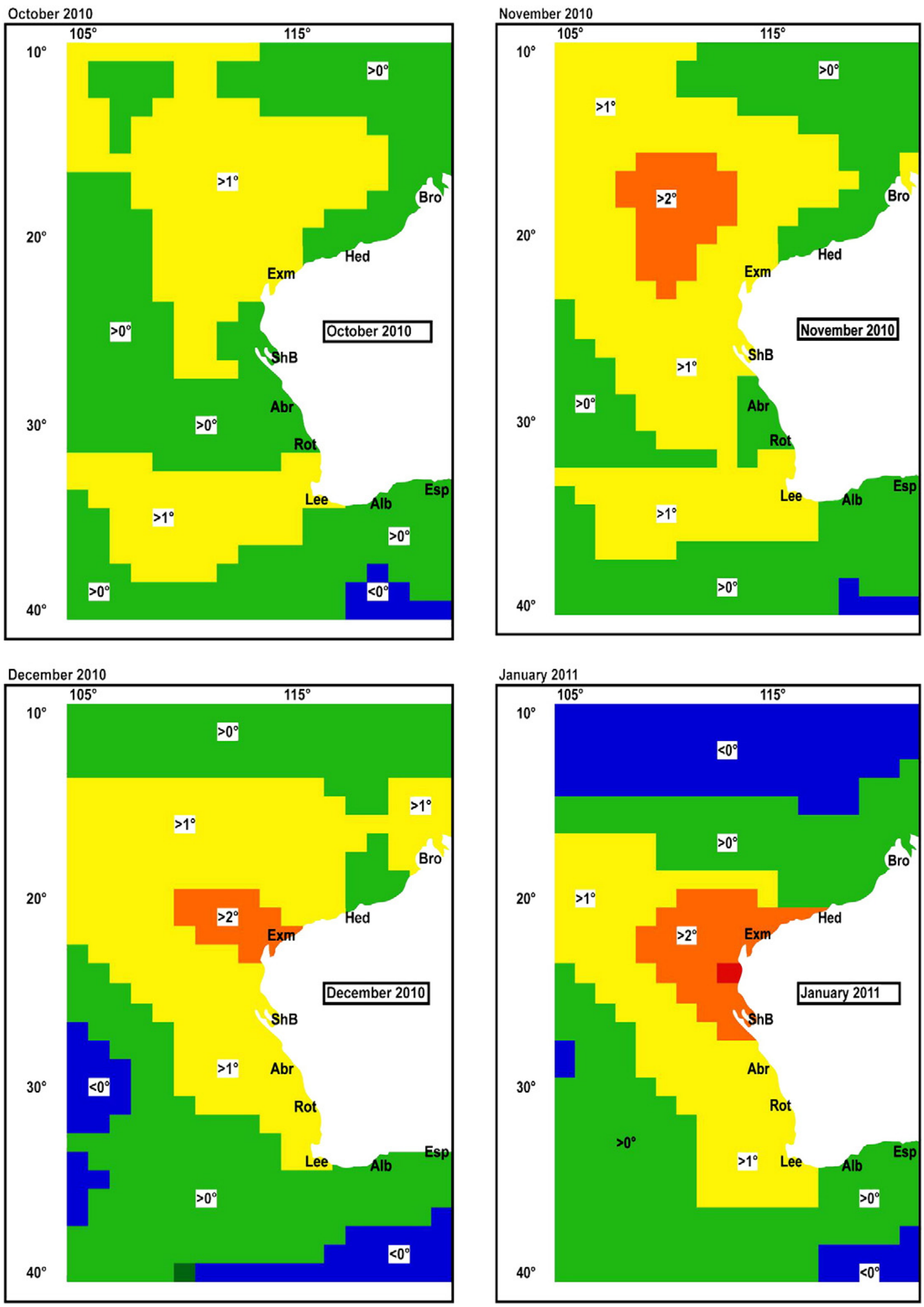

Fig. 2. Reynolds monthly SST anomaly charts for October 2010 to May 2011. Each block is nominally about 100∗100 km, and the anomalies have been derived from the long-term monthly means for each block. The location abbreviations are: Bro = Broome, Hed = Port Hedland, Exm = Exmouth, ShB = Shark Bay, Abr = Abrolhos Islands, Rot = Rottnest Island, Lee = Cape Leeuwin, Alb = Albany, and Esp = Esperance.

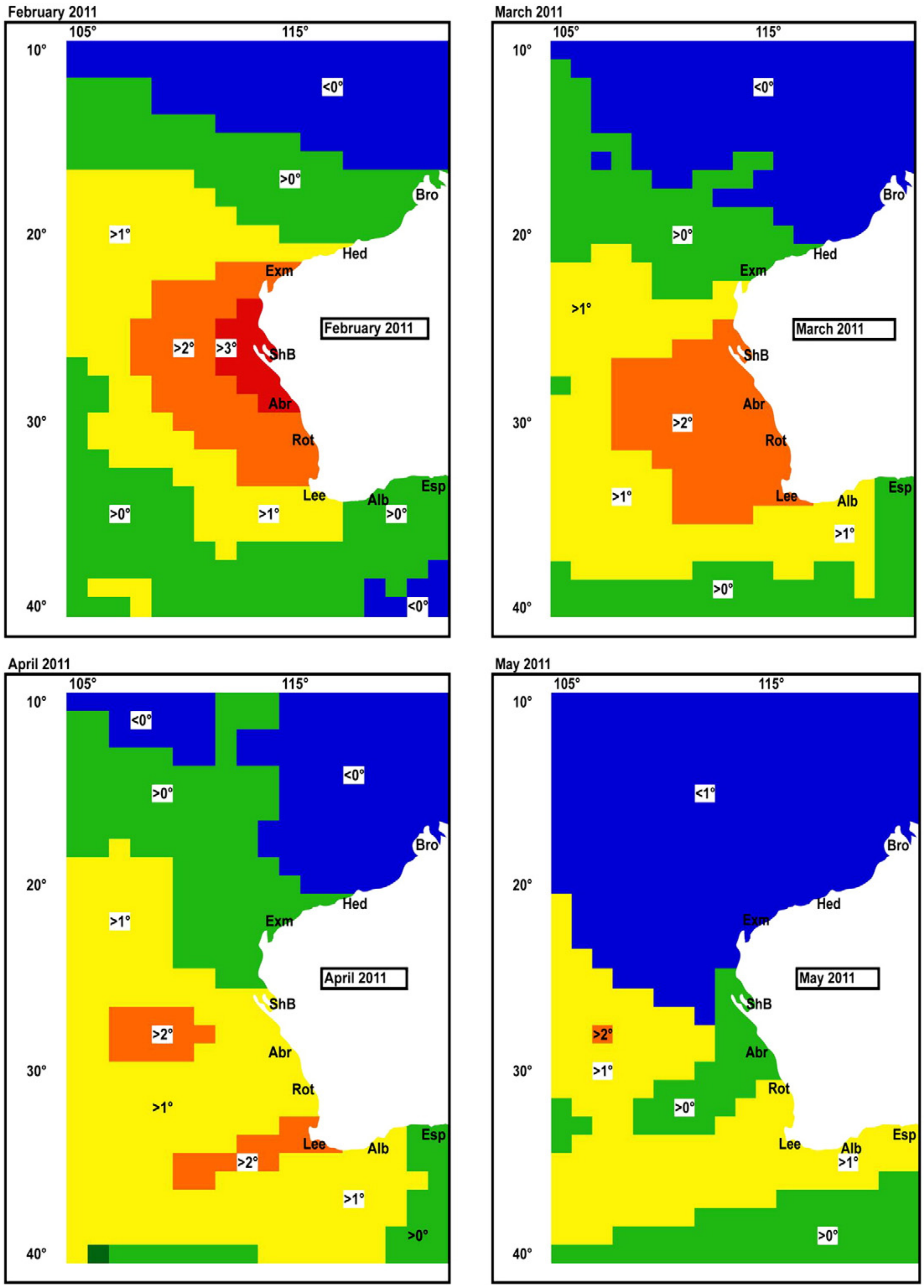

Fig. 2 (*continued*).

temperatures and anomalies were experienced at Port Gregory (28.9 °C, anomaly 5.0 °C), Dongara (29.4 °C, 5.1 °C), Rat Island (28.7 °C, 5.0 °C) and Jurien (28.3 °C, 5.6 °C) (Table 1). Even as far south as Busselton, the temperature anomaly reached 3.7 °C above the long-term average.

Superimposed on these daily-averaged temperatures was the diurnal cycle, which in the shallow nearshore waters had an amplitude of about 0.5 °C (approaching 1 °C on occasion) and peaked in the early afternoon — this would have further raised the actual temperatures for a few hours above the daily means shown in Fig. 4 and Table 1.

The effect of the heat wave was less pronounced along the south coast (Fig. 4; Table 1). The temperature at Hamelin Bay reached a peak of 24.0 °C on day 57 (26th February), and then 24.1 °C about a week later which approximately coincided with the peak higher up the west coast although less clearly defined. Interestingly, the peak temperature of 23.2 °C at Albany occurred on day 70 (11th March) while that further east at the Esperance jetty was 22.3 °C on day 58 (27th February), 2 weeks earlier than at Albany; the reason for this is not apparent.

Apart from the close timing of the peak temperatures, the general agreement in the temperature fluctuations along the west coast

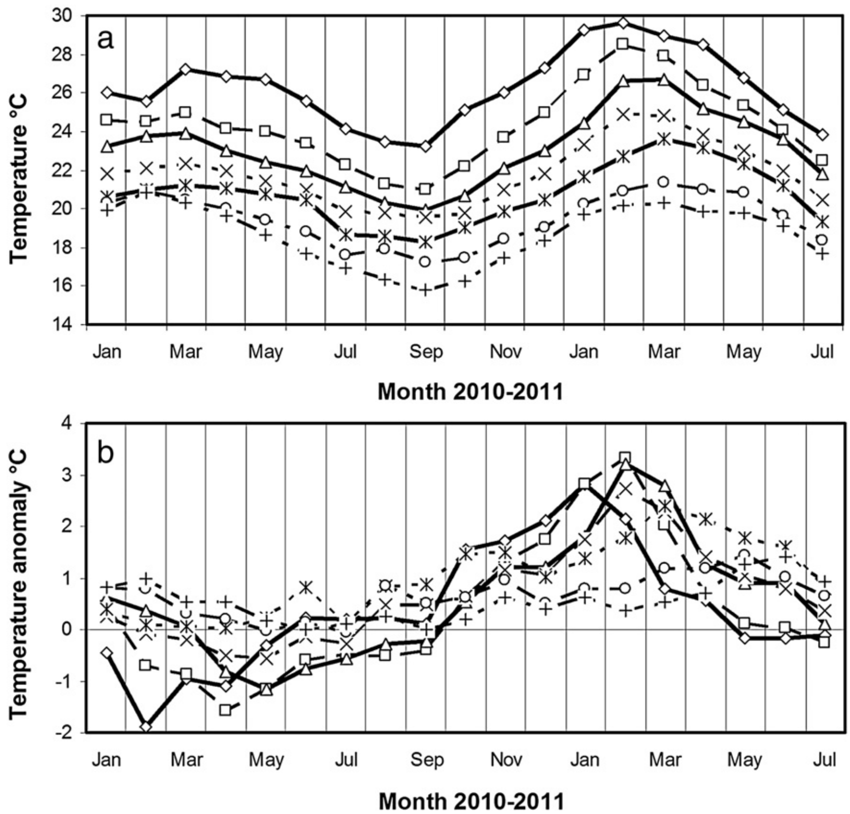

Fig. 3. (a) Reynolds monthly SSTs for 7 coastal blocks for the period January 2010 to July 2011; from north (warmest) to south (coolest) the sites were Exmouth (diamonds), Shark Bay (squares), Abrolhos Islands (triangles), Rottnest Island (crosses), Cape Leeuwin (asterisks), Albany (circles) and Esperance (plusses). The lines for the northern limit of the heat wave (Exmouth), the central peak area (Abrolhos) and the southern limit (Cape Leeuwin) have been bolded. (b) The corresponding Reynolds SST anomalies from the long-term monthly means.

between January and March is reflected in the high correlation between the daily temperatures at adjacent logger sites in Table 2. Up in the far north, the correlation between Coral Bay and its "neighbouring" stations was low, probably because the Exmouth logger was close inshore in Exmouth Gulf and therefore in a different water mass/current regime than Coral Bay, and the distance between Coral Bay and the next southern site at Port Gregory was over 500 km. Furthermore, the shelf topography was very different at these sites, and they are at the northern fringe of the heat wave. The correlation coefficients were above 0.8 for most pairs of sites between Port Gregory and Busselton, including the offshore islands, and the correlations between the daily temperatures at each site against Jurien (the "centre" of the heat wave in terms of the temperature anomaly — Table 1) were also over 0.8 (Table 3). This indicates a high level of spatial synchronicity along the west coast and suggests a larger-scale mechanism such as the air–sea heat flux (see Section 3.5) affecting all the sites simultaneously. Correlations with the south coast stations at Albany and Esperance were low as would be anticipated in view of the differing natures of the Leeuwin Current along the west and south coasts (Cresswell and Domingues 2009) and the fact that the air–sea heat flux component of the heat wave was largely restricted to the west coast (Section 3.5 and Fig. 10b).

The lagged correlations indicated that the daily temperatures from Coral Bay to Hamelin Bay were in phase with those at Jurien within a single day, with a hint that the southerly sites tended to lag Jurien by

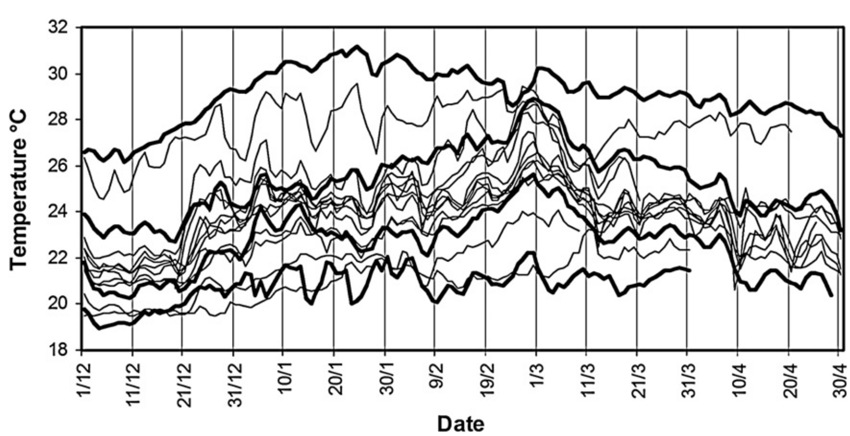

Fig. 4. Daily-averaged temperatures between December 2010 and April 2011 for selected temperature logger sites along the Western Australian coast. The 4 dark lines are (north to south) Exmouth, Port Gregory, Busselton and Esperance. The thin lines are for many of the other loggers listed in Table 1; individual sites have not been identified as the general agreement is clear.

Table 2
Correlation coefficients between the daily temperatures at selected adjacent pairs of coastal sites and between the offshore islands (Rat Island in the Abrolhos group and the "south" and "west" sites off Rottnest Island) between January and March 2011. The number of days available for the correlations is indicated in the last column. All correlations >0.27 are significant at the 1% level.

Site pairs	Correlation	No. of days
Coastal sites		
Exmouth–Coral Bay	0.435	90
Coral Bay–Port Gregory	0.123	90
Port Gregory–Dongara	0.822	80
Dongara–Jurien	0.943	80
Jurien–Lancelin	0.895	81
Lancelin–Alkimos	0.947	76
Alkimos–Hillarys	0.956	76
Hillarys–Warnbro Sound	0.765	75
Warnbro Sound–Busselton	0.916	75
Offshore islands		
Rat Island–Dongara	0.802	80
Rottnest (south)–Warnbro	0.804	75
Rottnest (south)–Rottnest (west)	0.952	90
Rat Island–Rottnest (south)	0.956	75

a day (with the exception of Warnbro and the estuarine site in the Peel–Harvey which were synchronous with Jurien).

3.3. Depth extent

Temperatures from the IMOS Two Rocks 50 m, 100 m and 150 m moorings were available until late March (when the mooring was retrieved) and from the 200 m mooring until May (ditto); they revealed both the depth of the warm layer and to some degree its offshore extent. Our discussion will focus on the near-surface mixed-layer temperatures rather than a detailed analysis of the dynamics and forcing of the vertical structure.

At the mid-shelf mooring (Fig. 5a), the water column was essentially well-mixed vertically (at least from the shallowest recorder at 25 m depth to near the seabed) throughout the December to March period. Following a daily-averaged peak of about 24 °C on day 31 (31st January) at the uppermost recorder, the temperature rose gradually to 2 higher peaks of 25.4 °C on days 59 (28th February) and 65 (6th March), and the high temperature anomalies were sustained for almost 10 days. These were similar to the temperatures at the Rottnest (west) loggers and the IMOS reference station (Table 1).

As would be expected, there was much more vertical structure at the deeper 100 m mooring (Fig. 5b), most of the "activity" being below 40 m, although for much of the time quasi-isothermal conditions prevailed. The peaks on days 31, 59 and 65 (31st January, 28th February and 6th March respectively) were all evident, during each of which the water column was effectively well mixed down to the sea bed. Intermittently, however, there were periods of appreciable stratification lasting a few days, with pulses of cooler water (typically 2–3 °C lower than the mixed layer temperature) probably welling up along the outer shelf from deeper offshore.

At the deeper 150 m station (Fig. 5c), the peak near-surface temperature at the end of February was about 1 °C higher than at the 100 m mooring (Table 1). Again the greatest thermal activity was below 50 m, and the periods of enhanced stratification were again associated with upwelling-like events similar to (but much greater than) those at the 100 m mooring. The largest vertical temperature difference was almost 7 °C in March.

The temperature structure at the 200 m mooring (Fig. 5d) was similar to that at the 150 m location, but with an even higher peak temperature – 27.0 °C on day 59 (28th February) – and greater vertical temperature differences due to the greater water depth. Overall, the surface temperature variability was highly synchronised across the shelf during this period.

Temperature profiles from the naval XBTs released just south of Perth in mid-March 2011 were mostly near the edge of the continental shelf in water depths varying from 50 m to 900 m. Although these profiles were taken about 2 weeks after the peak of the nearshore heatwave, the surface temperatures (not shown) were up to 25.4 °C and showed an almost isothermal mixed layer extending down to a well-defined thermocline at about 50 m depth, similar to the Two Rocks moorings.

3.4. Leeuwin Current

Coastal sea level can be used as an index of the "strength" of the Leeuwin Current, with higher sea levels at Fremantle being associated with a stronger current (which usually occurs during La Niña periods) and vice versa (Caputi et al., 2010; Feng et al., 2003; Pearce and Phillips, 1988). Stronger southward transport also tends to result in higher water temperatures along the shelf as the warm tropical waters are transported into temperate regions (Feng et al., 2008).

There is generally a close relationship between monthly values of the Southern Oscillation Index (SOI), Fremantle sea level anomaly

Table 3
Correlation coefficients between the daily temperatures at selected coastal sites and Jurien between January and March 2011. The 5 columns represent Jurien lagging by 2 days, by 1 day, zero (no lag/lead), leading by 1 day and by 2 days, respectively. The highest correlations at each site between Coral Bay and Hamelin Bay are bolded; adjacent lagged/leading days are also bolded where the correlations differ by ≤0.01.

Site	Lags by 2 days	Lags by 1 day	No lead or lag	Leads by 1 day	Leads by 2 days
Exmouth	−0.195	−0.128	−0.061	−0.040	−0.066
Coral Bay	0.327	0.361	**0.386**	0.305	0.129
Pt.Gregory	0.648	0.739	**0.808**	**0.806**	0.752
Rat Island	0.615	0.703	**0.755**	0.736	0.691
Rat Island	0.632	0.725	**0.811**	**0.812**	0.750
Pelsaert	0.547	0.625	**0.681**	**0.678**	0.636
Dongara	0.732	0.859	**0.943**	0.884	0.741
Jurien	0.725	0.889	**1.000**	0.888	0.724
Alkimos	0.580	0.733	**0.869**	0.857	0.730
Lancelin	0.622	0.764	**0.894**	**0.891**	0.769
Hillarys	0.574	0.681	0.800	**0.819**	0.726
Parker Point	0.544	0.667	0.818	**0.878**	0.830
Cockburn Snd (Mbs)	0.666	0.783	**0.906**	**0.906**	0.791
Warnbro	0.704	0.835	**0.923**	0.884	0.784
Peel-Harvey	0.568	0.697	**0.780**	0.688	0.480
Busselton Jetty	0.642	0.769	**0.861**	**0.865**	0.794
Hamelin Bay	0.629	0.694	0.751	**0.769**	0.745
Albany	−0.190	−0.163	−0.126	−0.100	−0.101
Esperance	0.189	0.243	0.201	0.126	0.083

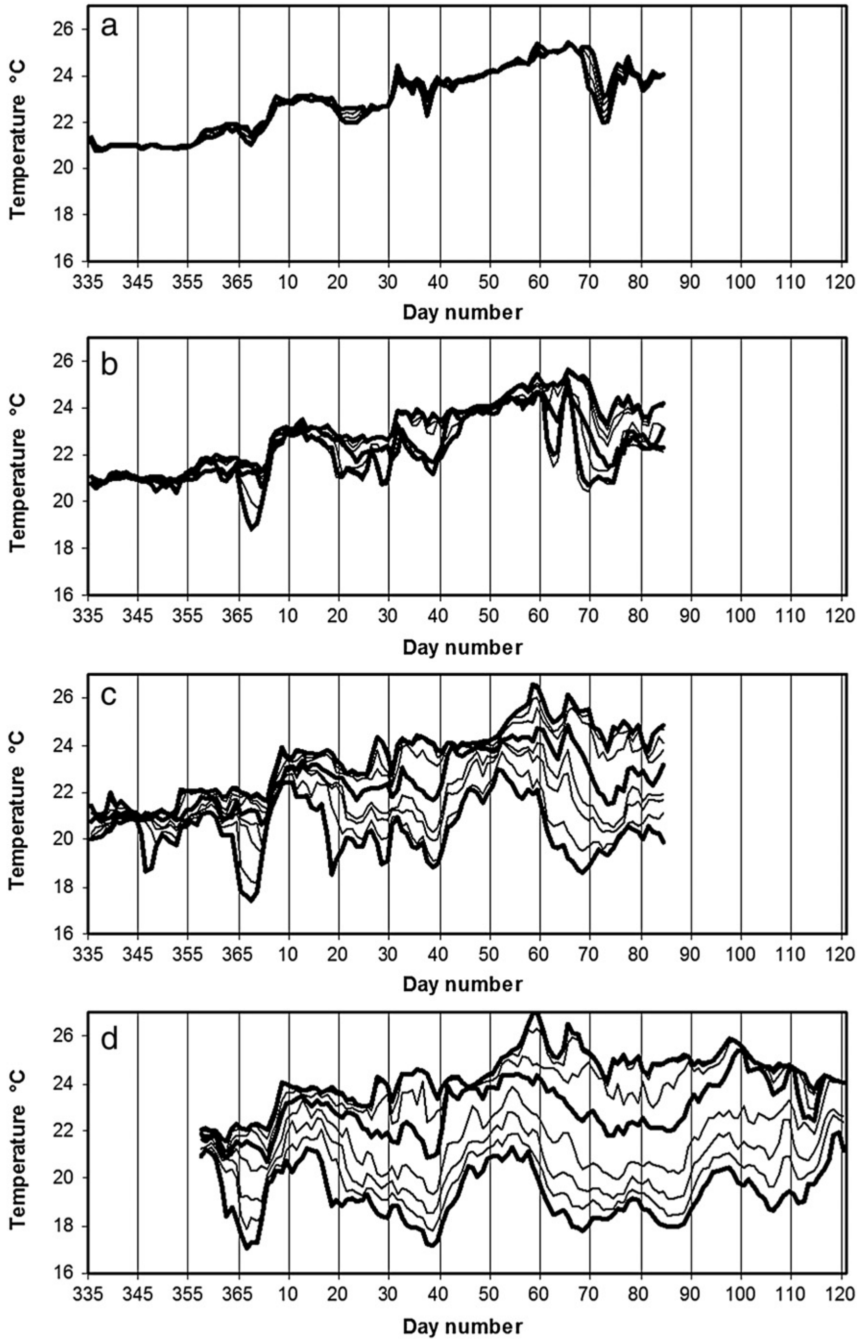

Fig. 5. Daily-averaged temperatures between December 2010 and April 2011 at the IMOS Two Rocks moorings; the near-surface, mid-depth and near-bottom temperatures have been bolded to assist interpretation. (a) the nominally 50 m (mid-shelf) mooring (instrument depths 25 m, 30 m, 35 m, 40 m and 46 m), (b) 100 m mooring (instruments at 25 m, 30 m, 35 m, 40 m, 50 m, 70 m, 90 m and 96 m), (c) 150 m mooring (instruments at 30 m, 49 m, 74 m, 84 m, 104 m, 124 m, 134 m, 144 m and 149 m) and (d) 200 m mooring (30 m, 40 m, 55 m, 75 m, 105 m, 130 m, 155 m and 180 m). The 50 m to 150 m moorings were recovered on 25th March, and the 200 m mooring was installed on 23rd December. The vertical scale has been fixed to aid comparison between the moorings.

(FMSLA) and the Reynolds sea-surface temperature anomaly (SSTA) (Fig. 6). Over the period 1982 to 2010, the correlations were:

FMSLA and SOI = 0.763
SOI and SSTA = 0.445
SSTA and FMSLA = 0.734

These are all significant at the 1% level.

The intensity of the summer 2011 warming episode was reflected by elevated values of the SOI, sea level and surface temperature (Fig. 6). It was the most extreme La Niña event experienced over the past 3 decades, indeed one of the 4 strongest of the past century (Anonymous, 2011; Beard et al., 2011); the monthly SOI values in October and December 2010 and also February and March 2011 were the highest ever recorded (Bureau of Meteorology, 2012). The event resulted in record high sea level anomalies as well as record high water temperatures off Western Australia — the Reynolds SST anomaly was by far the highest since the satellite records began in 1982 (Fig. 6; see also Wernberg et al., 2012).

The (smoothed) SOI began rising in early 2010, peaking at 20 to 25 between August 2010 and March 2011 before falling away into winter (Fig. 7); the Multivariate ENSO Index (not shown) displayed

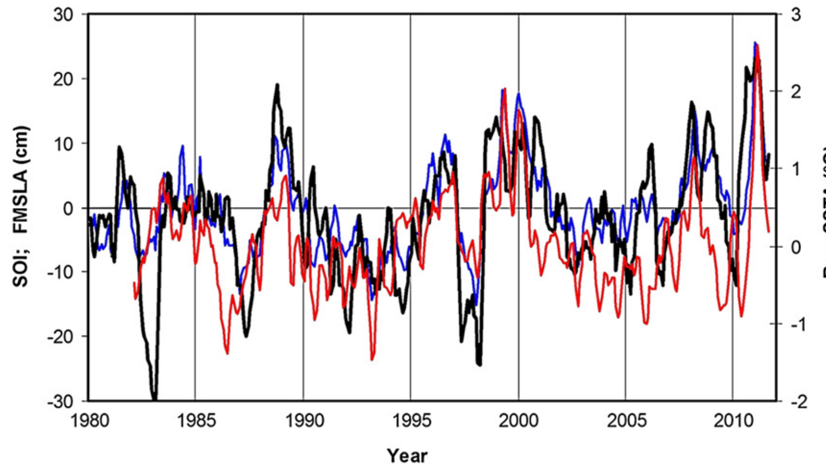

Fig. 6. Monthly values of the Southern Oscillation Index (SOI — black), sea level anomaly at Fremantle (FMSLA — blue) and the Reynolds SST anomaly for the block covering the Houtman Abrolhos Islands (ReynSSTA — red) from 1980 to 2011. Fremantle sea level has been linearly detrended to remove the long-term sea level rise. All values have been smoothed by a 3-point moving average to reduce small-scale variability.

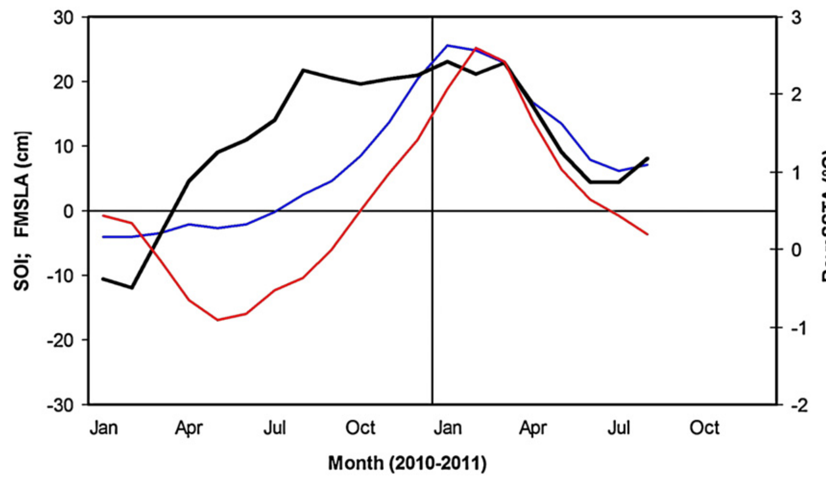

Fig. 7. As for Fig. 6, but showing more detail for 2010 and 2011.

similar variability. The sea level anomaly correspondingly rose from neutral levels to peak at a record high 25 cm in January 2011, implying a very strong Leeuwin Current, while the smoothed Reynolds SST anomaly reached record high values of over 2.7 °C in February and March 2011, eclipsing the previous record temperature anomaly of 2.0 °C in this area during the strong La Niña event in autumn 1999. Both the sea level and temperature anomalies thereafter returned to near-normal levels by June/July. As in Feng et al. (2003), most of the annual and interannual variations of the Fremantle sea level are due to steric height variability associated with the Leeuwin Current.

As a result of strengthened trade winds in the equatorial Pacific Ocean after mid-2010, upper ocean temperature and sea level anomalies in the western Pacific built up during the latter part of the year (Fig. 8) and were transmitted into the south-eastern Indian Ocean via

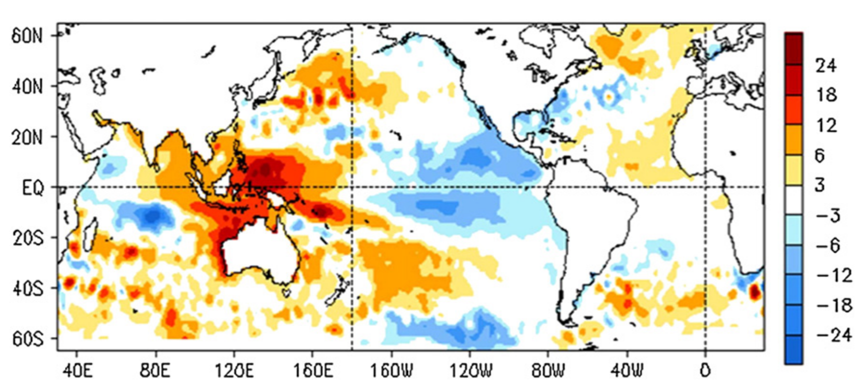

Fig. 8. Global sea level anomalies (cm) in February 2011 from the Global Ocean Data Assimilation System provided by the NOAA Climate Prediction Center.

the Indonesian Throughflow (Godfrey and Ridgway, 1985). The heat content of the upper 200 m of the SE Indian Ocean in December 2010 was much higher than in the previous December (Sandery, 2011; — see also Oliver and Thompson, 2011), in turn setting up the strong steric height gradient off Western Australia (Godfrey and Ridgway, 1985) and consequently the strong southward flow in the Leeuwin Current.

Satellite altimeter charts developed by CSIRO show the surface currents along the continental shelf and out into the open ocean. In mid-January (Fig. 9a), the Leeuwin Current was flowing southwards effectively along the edge of the continental shelf between Shark Bay and Cape Leeuwin, where it rounded the Cape and headed eastwards towards the Great Australian Bight. By 27th February (the peak of the heat wave) a mesoscale meander had developed off the Abrolhos Islands (29°S; Fig. 9b), bringing the warm water towards and onto the shelf at Dongara and Jurien Bay where the temperature peaked at 29.4° and 28.3 °C respectively (Table 1). A week later

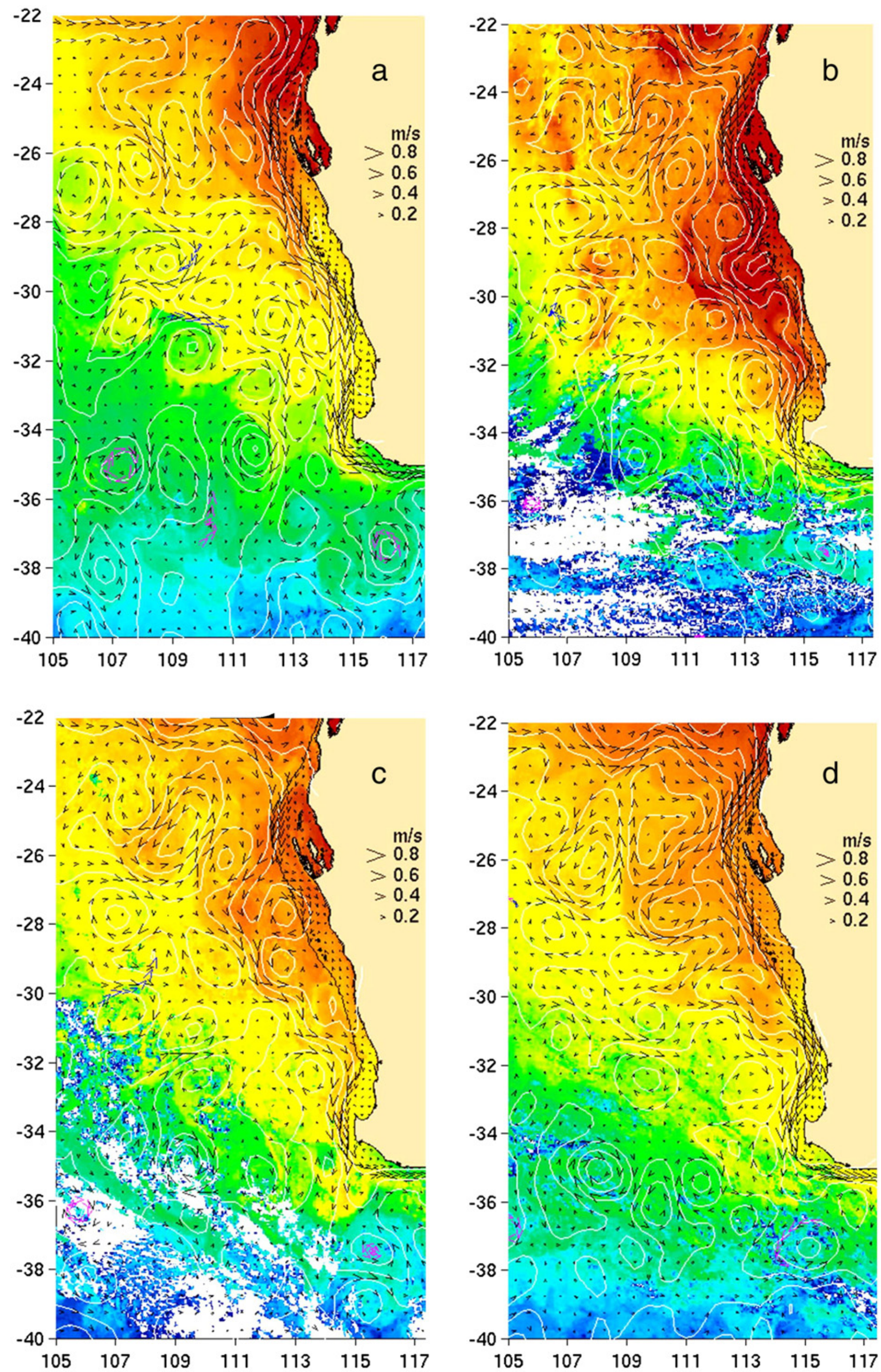

Fig. 9. Altimeter-derived surface geostrophic currents (arrows — note the speed scale in m s^{-1}) and sea surface temperatures (background colours) on (a) 11th January, (b) 27th February (the peak of the heat wave), (c) 6th March and (d) 27th March 2011. Highest temperatures are in red and coolest in blue. The black line marks the nominal edge of the continental shelf and the white lines are the sea surface topographic contours (0.1 m intervals). Acknowledgements to CSIRO Marine and Atmospheric Research (http://www.cmar.csiro.au/remotesensing/oceancurrents/SW/; accessed October 2011).

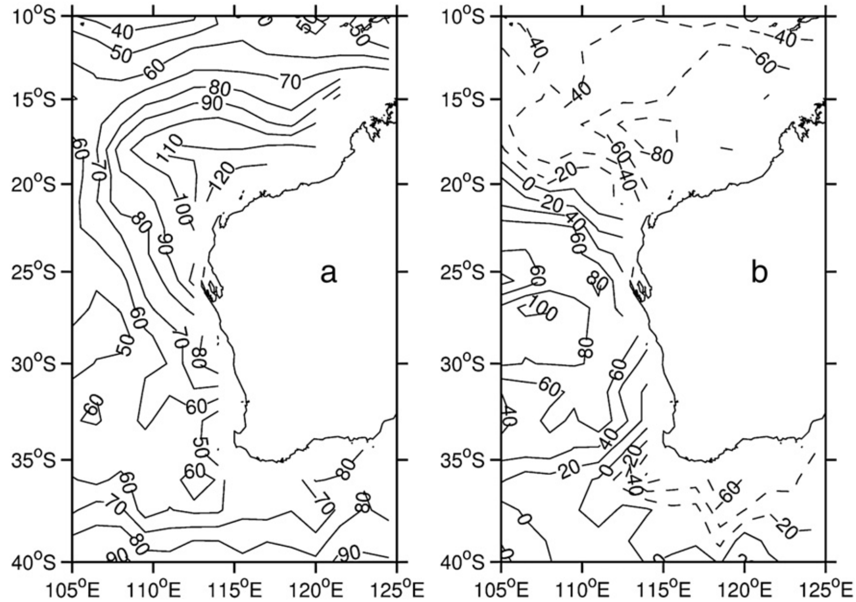

Fig. 10. (a) Average monthly heat flux into the ocean in February derived from the ECMWF-interim re-analysis between 2006 and 2010, and (b) the February 2011 heat flux anomaly from the longer-term mean. The contour interval is 10 W/m^2 — positive flux (solid contours) is downward heat flow into the ocean surface and negative flux (dashed) represents heat loss from the ocean.

(Fig. 9c), the Leeuwin Current was flowing well offshore of the shelf break all the way from Shark Bay to Perth, skirting the offshore boundaries of a series of meanders and eddies, and finally during March the flow was weakening (Fig. 7) as the Current returned to a position along the shelf break (Fig. 9d).

3.5. Air–sea heat flux and meteorological conditions

While the strong Leeuwin Current brought warmer water southwards along the continental shelf and mesoscale meanders/eddies contributed to the observed regional warming centred on the Dongara/Jurien region (as described previously), the near-synchronous nature of the heat wave along the coast (Table 1) indicates that another large-scale mechanism was also influencing the water temperatures.

Typically, there is a net heat input into the southeastern Indian Ocean during February (Fig. 10a). However, the air–sea heat flux anomaly in February 2011 was strongly positive, indicating unusually high oceanic heat gain over the large area from Ningaloo down to the Capes region (Fig. 10b). This was centred between 25° and 30°S, effectively matching the observed extent and distribution of the peak temperatures (Fig. 2b and Table 1). North of Ningaloo and south of Geographe Bay, the heat flux anomaly was negative (i.e. the heat flux into the ocean was lower than the long-term February average) and the surface temperature anomalies in those regions were correspondingly within normal limits. Although the peak of the heat flux anomaly was well offshore at 107°E (Fig. 10b), the largest temperature anomalies were experienced nearer the coast because of the advection of warmer water along the shelf break by the Leeuwin Current and the shallowness of the water on the continental shelf.

There was a strong seasonal pattern in the area-averaged heat flux over the area 22° to 33°S, 110°E to the coast (Fig. 11a), with positive values (oceanic heat gain through the water surface) during the summer months and a much larger heat loss between about April and September each year. The heat flux anomaly from the long-term average in February 2011 was very high (Fig. 11b), standing out as a single monthly "spike" above the January and March values.

The daily heat fluxes (Fig. 12b) were strongly and consistently positive at 100 to 200 W/m^2 during February 2011, the period when the water temperatures along the coast were rising, before suddenly reversing to net daily heat loss from the ocean in early March. Thereafter, the flux oscillated between positive and negative for the rest of the month.

The temperature rise purely from heat gain at the surface is given by:

$$\Delta T = Q/(H * \rho * Cp) \;\; ^\circ C/s$$

where

Q	heat input (W/m^2)
H	water depth or mixed layer depth (m)
ρ	water density (~1025 kg/m^3) and
Cp	specific heat of water (4200 J/kg/°C)

In shallow nearshore waters, a daily heat input of 150 W/m^2 mixed down through a water depth of 20 m would result in a temperature rise of about 0.15 °C/day, or 3 °C in 3 weeks — consistent with the measured temperature rise of 3 °C along the inner shelf during February in Fig. 12a. A lower warming trend at the offshore moorings during the same period (Fig. 5) is also consistent with the greater mixed layer depth there (~50 m — see Section 3.3) and with mixing and advection processes that tended to balance the heat input. (A complete ocean heat budget analysis would be required to separate the effects of Leeuwin Current advection and surface heat flux, and has not been undertaken here). Correlation of the daily water temperatures against the daily heat flux values in February/March gave coefficients of between 0.5 and 0.8 with lags varying between 3 and 8 days at different sites.

Complementing the heat fluxes with the daily winds and air temperatures at the offshore islands (North Island, in the Abrolhos Islands group, and Rottnest Island) clarifies some of the atmospheric processes controlling the nearshore water temperatures (Fig. 12). Meteorological conditions at Rat Island and Rottnest Island over the 60-day period February/March were very similar. There was a high correlation between the winds at the 2 sites (northward components 0.798, eastward

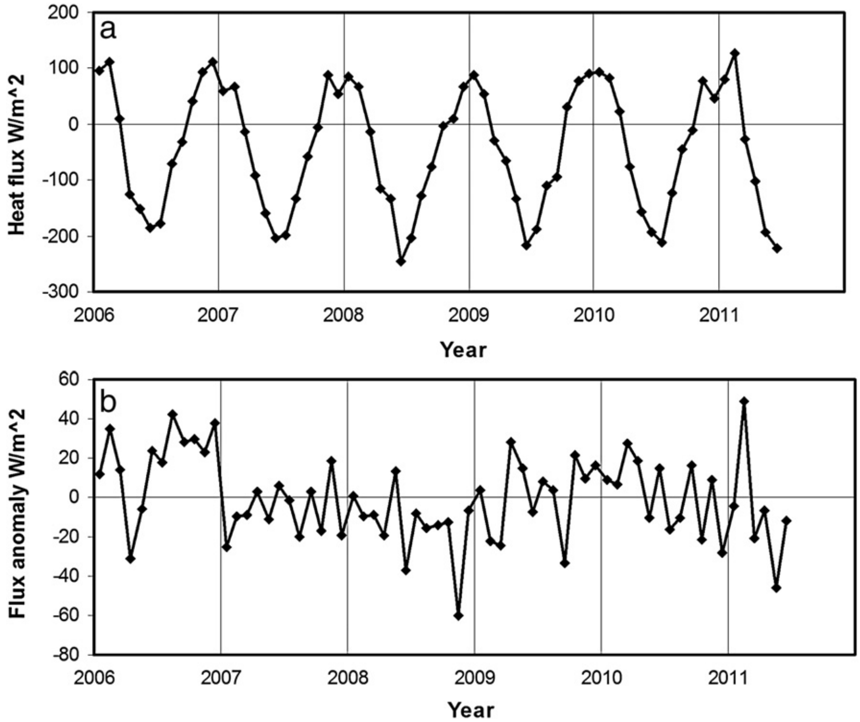

Fig. 11. a) Monthly mean total heat flux (W/m^2) into the heat ocean over the area 22° to 33°S, 110°E to the coast, between 2006 and early 2011. b) The heat flux anomalies from the 2006–2010 mean annual cycle.

components 0.523; Fig. 12c and d respectively) and the air temperatures (0.853; Fig. 12f), all significant at the 1% level and indicating a high level of consistency in the environmental conditions on the continental shelf during the peak of the heat wave. The major features of the wind fields matched well and were similar in magnitude, although the eastward (onshore–offshore) components were somewhat stronger eastward at Rottnest Island than at the Abrolhos.

The wind speed progressively decreased (albeit with some few-day variability) from about 10 m/s at the start of February to almost calm by the end of the month (Fig. 12e), followed by a burst of southerly wind on day 64 (5th March) — coinciding with the sharp reversal from oceanic heat gain to heat loss. The highest air temperature (Fig. 12f) occurred at North Island on day 60 (coinciding with the peak water temperatures — Fig. 12a), while the air temperatures at Rottnest were 2° to 4 °C lower and peaked on the previous day. The correlation between the daily water temperatures at the northern/mid-west sites Rat Island, Dongara and Jurien against the air temperature at North Island were (respectively) 0.725, 0.696 and 0.669, while that between the sea temperatures at the more southerly locations of Lancelin, Alkimos and Cockburn Sound (site MBS) and the Rottnest Island air temperatures were marginally lower at 0.461, 0.446 and 0.547 — these are still significant at the 1% level. The relatively calm conditions were reflected in an unusually low wave height at the wave-rider buoy off Rottnest Island in early 2011 (unpublished data, Western Australian Department of Transport). The monthly mean significant wave height in February 2011 was only 1.3 m compared with the long-term mean of 1.74 m, and this was in fact the lowest monthly significant wave height in the record 2004 to mid-2011.

The important role of the air–sea heat flux is supported by the fact that semi-enclosed water bodies such as Cockburn Sound and (especially) the Peel–Harvey system, having restricted exchange with the open ocean, nevertheless experienced the peak temperatures at the same time as the coastal and island waters (Table 1 — note that the temperature anomaly in the shallow Peel estuary was 5.2 °C, much higher than that in the adjacent open ocean). Likewise, weekly sampling in the Swan River estuary (which enters the sea at Fremantle, near Perth — Fig. 1) showed the progression of water temperatures in early 2011 as (peak values bolded):

Date	Lower Swan	Middle Swan	Upper Swan
14 Feb	23.5–24.7 °C	24.4–26.7 °C	24.8–28.4 °C
21 Feb	24.7–25.1 °C	25.6–25.9 °C	25.9–27.6 °C
28 Feb	25.8–29.5 °C	29.1–31.5 °C	28.4–31.9 °C
8 Mar	24.6–25.5 °C	25.1–26.5 °C	25.6–27.3 °C
14 Mar	23.0–24.0 °C	23.0–24.8 °C	23.7–25.4 °C

Source: Swan River Trust website: http://www.swanrivertrust.wa.gov.au/science/river/Vertical%20plots%20archive/swanrivervp2011.aspx (accessed August 2011).

The highest temperatures of almost 32 °C occurred on the 28th February in the upper reaches of the Swan estuary, well away from direct exchange with the ocean, indicating that heat flux from the atmosphere was the driving mechanism rather than advection of warm water up the estuary.

Although the focus of this paper is on the heat wave conditions, it may be noted that the correlations between the daily subsurface water temperatures at the IMOS moorings (Fig. 5) and the alongshore wind components at Rottnest Island over the central period of the heat wave (February/March) were dominantly negative, consistent with a wind-driven upwelling process bringing cooler water towards the shelf at depth in association with stronger southerly winds. The maximum correlations down the water column occurred near the seabed at the shallowest mid-shelf mooring, and at 70 m depth at the deeper offshore sites, ranging between −0.48 and −0.70 and lagging the wind by about 4 days — the correlations were all significant at the 1% level. The apparent vertical phase propagation may have

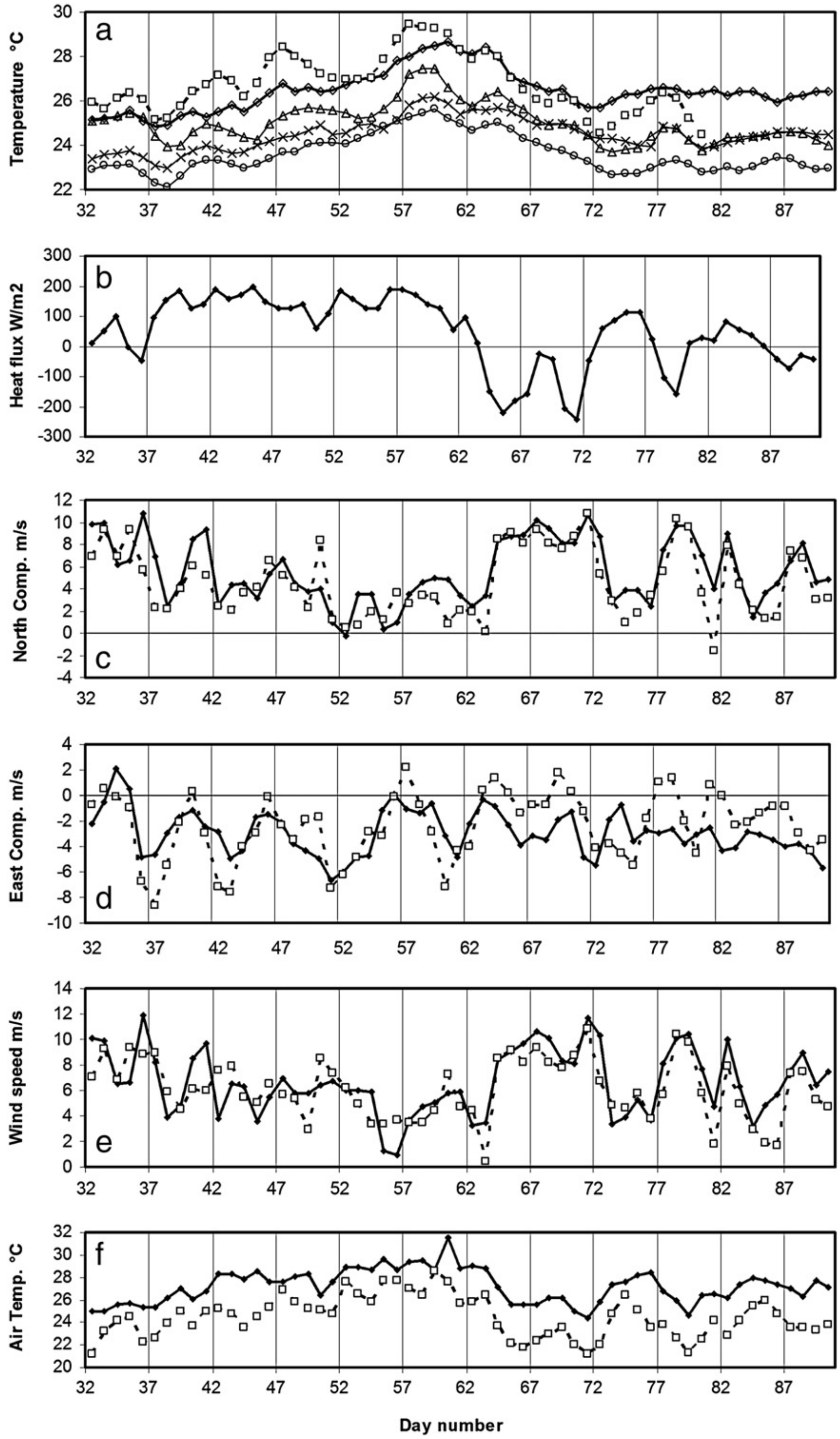

Fig. 12. (a) Daily mean water temperatures at selected locations along the Western Australian coast at Rat Island (diamonds, thick line), Dongara (squares, dashed line), Lancelin (triangles), Rottnest Island (x's) and Busselton (diamonds, thin line) between 1st February and 31st March, the 2-month period spanning the peak of the heat wave. (b) Total daily heat flux into the ocean (positive), averaged over the area 22° to 33°S, 110°E to the coast. (c) to (f) Meteorological conditions at the Abrolhos Islands (North Island, solid line) and Rottnest Island (dotted line and open symbols) for (c) northward wind component, (d) eastward (onshore) wind component, (e) wind speed and (f) air temperature.

been due to a combination of remote and locally forced temperature variations.

4. Implications for mortality and range extensions

The heat wave resulted in the mortality of many fish and invertebrate species, and there were also many observations of tropical fish much further south than their normal distributions.

4.1. Fish and invertebrate mortality

The most devastating of the mortality events was the virtually complete annihilation of the abalone (*Haliotis roei*) fishery at Kalbarri (de Lestang and Hart, 2011). In early February, industry divers reported that the abalone stocks were stressed although in high abundance, but by early March (just after the peak of the heat wave, when the temperatures at Port Gregory and Dongara were peaking at about 29 °C — Table 1), there was a complete mortality of abalone stocks north of the Murchison River (Kalbarri). Lobster mortalities were observed at the Abrolhos Islands and Leeman (de Lestang and Hart, 2011), with reports of lobsters being docile and away from protected areas (Evans and Bellchambers, 2011).

More widespread, although perhaps not as devastating, was the bleaching of corals between the Montebello Islands (north of Exmouth) and Rottnest Island in the south (Moore et al., submitted for publication), which can be attributed to the progressive warming of the nearshore waters in early summer, culminating in the peak temperatures at the end of February. Although the "centre" of the heat wave was in the vicinity of Dongara, the Abrolhos Islands and Jurien where the temperature anomalies exceeded 5 °C (Table 1), elevated temperatures extended at least as far as north as Coral Bay (no anomaly calculated but the peak temperature approached 30 °C) and south to Busselton (anomaly 3.7 °C). Local observations in the Easter Group of the Abrolhos Islands found that up to 80% of the corals had been bleached in some areas (Evans and Bellchambers, 2011; see also Smale and Wernberg, 2012), and extensive bleaching of corals at Rottnest Island was also reported (Thomson et al., 2011) with temperatures exceeding 26 °C at the peak of the heat wave. There were major impacts on seaweeds and invertebrates at Jurien and Hamelin Bay as well (Wernberg et al. 2012).

Reports of fish kills were widespread (Pearce et al., 2011), and there was no evidence that a pathogen was involved (Jones, 2011), the spike in water temperatures in conjunction with calm wave conditions being the likely cause. Fish mortality was observed at many locations between Shark Bay and Albany (Smith et al., 2011), where hundreds of elongate sunfish *Ranzania laevis* were washed up on local beaches, reminiscent of the similar mortality during the strong La Niña event in autumn 2008 (Smith et al., 2010) when the Leeuwin Current was again anomalously strong and sea temperatures were much higher than usual (Fig. 6).

By contrast with the mortality observed in some locations, there were positive outcomes of the elevated temperatures in others, such as greatly increased king prawn (*Penaeus latisulcatus*) recruitment and catchability in Shark Bay (Sporer and Kangas, 2011). Similarly, tiger prawn (*Penaeus esculentus*) catches in Exmouth Gulf in early 2011 were much higher than in the previous year, attributed by Sporer and Kangas (2011) to the higher temperatures of over 30 °C encountered there.

4.2. Temporary range extensions

As pointed out by Smith et al. (2011), sightings of tropical species (such as whale sharks and manta rays) well south of their traditional ranges may not be permanent range extensions in the usual sense but were a direct consequence of the elevated water temperatures and the strong southward flow in the Leeuwin Current during the heat wave.

While the normal temperature range in which whale sharks are found is believed to be 21 to 26 °C (Taylor, 1994), sharks studied more recently off Ningaloo Reef spent most of their time in water with temperatures between 23 and 28 °C (Wilson et al., 2006). Previously, whale sharks have been sighted off Shark Bay (south of their normal range — Colman, 1997, cited in Wilson et al., 2001) including a stranded juvenile (Speed et al., 2009), but during the heat wave there were a number of whale shark and manta ray sightings well south of Shark Bay, including off Cheynes Beach near Albany (Pearce et al. 2011). The presence of such large fish so far south is probably not directly attributable to transport in the Leeuwin Current because of their strong swimming capability, so it is more likely that the warmer water and southward transport of the planktonic krill (*Pseudeuphausia latifrons*, which forms a substantial part of the whale shark diet — Taylor, 1994) would be responsible.

The presence of tropical fish (larvae, juveniles and adults) has previously been observed in the nearshore waters of Rottnest Island and attributed to southward transport in the Leeuwin Current (Hutchins, 1991; Hutchins and Pearce, 1994; Pearce and Hutchins, 2009). During the 2010/2011 summer heat wave, however, recruitment of some species at the Island was exceptionally high (Hutchins, 2011). A variety of new species were observed for the first time, and the abundance of the commonly-seen scissor-tail sergeant *Abudefduf sexfasciatus* was at record high levels, particularly in the sanctuary zone at Parker Point on the south-east coast of the Island. Historically, Rottnest Island was the furthest south the sergeants had previously been found, but a juvenile scissor-tail was sighted for the first time down at Busselton Jetty at the peak of the heat wave (Micha, 2011).

5. Conclusions

During the summer months of 2010/2011, near-record strength La Niña conditions were prevailing. These were associated with an anomalously high sea level anomaly in the equatorial western Pacific Ocean. The resulting strong Leeuwin Current, combined with unusually high air–sea heat flux into the ocean, resulted in the highest sea surface temperatures off south-western Australia on record.

This unprecedented warming, which is being viewed as a major few-week event superimposed on the underlying longer-term global temperature rise, had some substantial consequences for the fish and marine invertebrates along the continental shelf. Fortunately, a very good set of temperature records was available from monitoring sites along much the Western Australian coast and offshore islands, enabling the growth and decay of the heat wave to be elucidated. The availability of such information amply demonstrates the value of ongoing oceanographic monitoring programmes in coastal waters.

On the larger scale, satellite-derived sea surface temperatures showed the development of the warm water from northwest of Exmouth at the end of 2010 to cover the entire south-western shelf and offshore region between Exmouth and the Capes area (Fig. 1) in early 2011. Air–sea heat flux estimates revealed that there was an anomalously high heat input into the ocean in February, centred on the central mid-west region, effectively matching the latitudinal range of the warm waters. The peak daily water temperatures along the continental shelf occurred at the end of a lengthy spell of well above-average heat flux into the ocean.

This large-scale heat flux explains the near-synchronicity of the nearshore temperatures recorded by hourly/daily temperature logging at numerous sites along the coast (and indeed some semi-enclosed water bodies such as the Peel–Harvey estuary and the Swan River), which showed that the local effects peaked over about a week from 27th February to 4th March. While advection by the strong Leeuwin Current and a strong heat input to the ocean across the air–sea interface both contributed to the warming event, the relative contributions of these 2 mechanisms to the heat wave require further research.

Some of the consequences of the heat wave on the marine biota were equally unprecedented. These ranged from widespread fish and invertebrate mortality to some interesting (albeit probably temporary) range extensions of both megafauna (specifically whale sharks and manta rays) and tropical fish recruiting to southern waters.

It is possible that major warming events of this nature will occur from time to time in the future, and this heat wave demonstrated some of the potential implications for the local marine ecology and fisheries.

Acknowledgements

This work was partly supported by the CSIRO Wealth from Oceans Flagship, the Western Australian Marine Science Institution (WAMSI), the Integrated Marine Observing System (IMOS), the Fisheries Research and Development Corporation (FRDC) and the Western Australian Department of Fisheries.

We are indebted to our colleagues for their generous provision of temperature data: Mark Rossbach and Chris Marsh (Department of Fisheries, for the puerulus and Cockburn Sound logger temperatures respectively), Alex Hoschke (Curtin University, for Exmouth and Rottnest temperatures), Kimberly Marrs Ekamper (Murdoch University, for Lancelin data), Damian Thomson (CSIRO, for Rottnest temperatures), Anna Micha (Busselton Jetty Environment and Conservation Association, for Busselton temperatures), Thomas Wernberg (University of Western Australia, for Hamelin Bay), and the Fisheries Research and Development Corporation (FRDC, with Erica Starling, Craig Koltasz and Klaas Hartmann, for the Abrolhos Islands temperatures). Ian Darby and Mark Snell (CSIRO) processed the Integrated Marine Observing System (IMOS) temperatures, the Bureau of Meteorology provided the Seaframe monitoring temperatures and Steven Moyes (Western Australian Department of Transport) sent us the Albany Wave-rider buoy temperatures. The Reynolds SSTs were processed by Ken Suber (CSIRO), and the Royal Australian Navy (Luke Callcut) provided the XBT profiles. Yan Xue (NOAA) provided the global sea level maps.

The wind data for Rottnest Island and North Island were acquired through the Australian Bureau of Meteorology (Glenn Cook and Yanhui Blockley), while wave data off Rottnest Island were provided by the WA Department of Transport (Steven Moyes and Tony Lamberto).

Finally, we appreciate the assistance of Marianna Zakrzewski and Sandy Clarke (both Department of Fisheries) for preparation of Figs. 1 and 2 respectively.

References

Anonymous, 2011. Frequent heavy rain events in late 2010/early 2011 lead to widespread flooding across eastern Australia. Bull. Aust. Met. Oceanogr. Soc. 24, 22–30.

Beard, G., Chandler, E., Watkins, A.B., Jones, D.A., 2011. How does the 2010–2011 La Niña compare with past La Niña events? Bull. Aust. Met. Oceanogr. Soc. 24, 17–20.

Black, E., Blackburn, M., Harrison, G., Hoskins, B., Methven, J., 2004. Factors contributing to the summer 2003 European heatwave. Weather 59, 217–222.

Bureau of Meteorology, 2012. Record-breaking La Niña events: an analysis of the La Niña life cycle and the impacts and significance of the 2010–11 and 2011–12 La Niña events in Australia. http://www.bom.gov.au/climate/enso/history/ln-2010-12/?ref=ad.

Byrne, M., 2011. Impact of ocean warming and ocean acidification on marine invertebrate life history stages: vulnerabilities and potential for persistence in a changing ocean. Oceanogr. Mar. Biol. Annu. Rev. 49, 1–43.

Caputi, N., Chubb, C., Pearce, A., 2001. Environmental effects on recruitment of the western rock lobster, *Panulirus cygnus*. Mar. Freshw. Res. 52, 1167–1174.

Caputi, N., de Lestang, S., Feng, M., Pearce, A., 2009. Seasonal variation in the long-term warming trend in water temperature off the Western Australian coast. Mar. Freshw. Res. 60, 129–139.

Caputi, N., Melville-Smith, R., de Lestang, S., Pearce, A., Feng, M., 2010. The effect of climate change on the western rock lobster (*Panulirus cygnus*) fishery of Western Australia. Can. J. Fish. Aquat. Sci. 67, 85–96.

Chittleborough, R.G., 1975. Breeding of *Panulirus longipes cygnus* George under natural and controlled conditions. Aust. J. Mar. Freshwat. Res. 27, 499–516.

Clarke, A.J., Li, J., 2004. El Nino/La Niña shelf edge flow and Australian western rock lobsters. Geophys. Res. Lett. 31 http://dx.doi.org/10.1029/2003GLO18900 (4 pp.).

Colman, J., 1997. Whale shark interaction management, with particular reference to Ningaloo Marine Park: 1997–2007. Western Australian Department of Conservation and Land Management, Wildlife Management Program No.27. (63 pp.).

Cresswell, G.R., Golding, T.J., 1980. Observations of a south-flowing current in the southeastern Indian Ocean. Deep-Sea Res. 27A, 449–466.

Cresswell, G.R., Domingues, C., 2009. The Leeuwin Current south of Western Australia. J. R. Soc. West. Aust. 92, 83–100.

Cropp, D., Koltasz, C., Boschetti, P., Davidson, M., 2011. Develop the non-maxima pearl industry at the Abrolhos Islands (*Pinctada imbricata*). Unpublished Final Report on FRDC Project 2007/216, Latitude Fisheries Pty Ltd, Geraldton, Western Australia, 181 pp.

Dee, D.P., Uppala, S.M., Simmons, A.J., Berrisford, P., Poli, P., Kobayashi, S., Andrae, U., Balmaseda, M.A., Balsamo, G., Bauer, P., Bechtold, P., Beljaars, A.C.M., van de Berg, L., Bidlot, J., Bormann, N., Delsol, C., Dragani, R., Fuentes, M., Geer, A.J., Haimberger, L., Healy, S.B., Hersbach, H., Holm, E.V., Isaksen, L., Kallberg, P., Kohler, M., Matricardi, M., McNally, A.P., Monge-Sanz, B.M., Morcrette, J.-J., Park, B.-K., Peubey, C., de Rosnay, P., Tavolato, C., Thepaut, J.-N., Vitart, F., 2011. The ERA-Interim reanalysis: configuration and performance of the data assimilation system. Q. J. R. Meteorol. Soc. 137, 553–597.

de Lestang, S., Hart, A.M., 2011. Lobster and abalone mortalities. In: Pearce, A.F., Lenanton, R., Jackson, G., Moore, J., Feng, M., Gaughan, D. (Eds.), The 'Marine Heat Wave' Off Western Australia during the Summer of 2010/2011. : Dept. Fish. West. Aust. Res. Rept., 222. Department of Fisheries, Western Australia, pp. 11–12.

Evans, S., Bellchambers, L., 2011. Observations on the effects high water temperatures at the Houtman Abrolhos Islands. In: Pearce, A.F., Lenanton, R., Jackson, G., Moore, J., Feng, M., Gaughan, D. (Eds.), The 'Marine Heat Wave' Off Western Australia during the Summer of 2010/2011. : Dept. Fish. West. Aust. Res. Rept., 222. Department of Fisheries, Western Australia, p. 13.

Feng, M., Biastoch, A., Boning, C., Caputi, N., Meyers, G., 2008. Seasonal and interannual variations of upper ocean heat balance off the west coast of Australia. J. Geophys. Res. 113, C12025 http://dx.doi.org/10.1029/2008JC004908.

Feng, M., Meyers, G., Pearce, A., Wijffels, S., 2003. Annual and interannual variations of the Leeuwin Current at 32°S. J. Geophys. Res. 108 (C11), 3355 http://dx.doi.org/10.1029/2002JC001763.

Godfrey, J.S., Ridgway, K.R., 1985. The large-scale environment of the poleward-flowing Leeuwin Current, Western Australia: longshore steric height gradients, wind stresses and geostrophic flow. J. Phys. Oceanogr. 15, 481–495.

Hobbs, J.P.A., McDonald, C.A., 2010. Increased seawater temperature and decreased dissolved oxygen triggers fish kill at the Cocos (Keeling) Islands, Indian Ocean. J. Fish Biol. 77, 1219–1229.

Hutchins, J.B., 1991. Dispersal of tropical fishes to temperate seas in the Southern Hemisphere. J. R. Soc. West. Aust. 74, 79–84.

Hutchins, J.B., 2011. Enhanced larval fish recruitment at Rottnest Island. In: Pearce, A.F., Lenanton, R., Jackson, G., Moore, J., Feng, M., Gaughan, D. (Eds.), The 'Marine Heat Wave' Off Western Australia during the Summer of 2010/2011. : Dept. Fish. West. Aust. Res. Rept., 222. Department of Fisheries, Western Australia, p. 14.

Hutchins, J.B., Pearce, A.F., 1994. Influence of the Leeuwin Current on recruitment of tropical reef fishes at Rottnest Island, Western Australia. Bull. Mar. Sci. 54, 245–255.

Jones, B., 2011. Dead fish — simmered or chilled? In: Pearce, A.F., Lenanton, R., Jackson, G., Moore, J., Feng, M., Gaughan, D. (Eds.), The 'Marine Heat Wave' Off Western Australia during the Summer of 2010/2011. : Dept. Fish. West. Aust. Res. Rept., 222. Department of Fisheries, Western Australia, p. 8.

Kim, K.H., Hwang, Y.J., Kwon, S.R., 2001. Influence of daily water temperature changes on the chemiluminescent response and mortality of cultured rockfish (*Sebastes schlegeli*). Aquaculture 192, 93–99.

Kim, W., Yeh, S.-W., Kim, J.-H., Kug, J.-S., Kwon, M., 2011. The unique 2009–2010 El Nino event: a fast phase transition of warm pool El Nino to La Niña. Geophys. Res. Lett. 38, L15809 http://dx.doi.org/10.1029/2011GL048521.

Lenanton, R.C., Caputi, N., Kangas, M., Craine, M., 2009. The ongoing influence of the Leeuwin Current on economically important fish and invertebrates off temperate Western Australia — has it changed? J. R. Soc. West. Aust. 92 (2), 111–127.

Lenanton, R.C., Joll, L., Penn, J., Jones, K., 1991. The influence of the Leeuwin Current on coastal fisheries of Western Australia. Proceedings of the Leeuwin Current Symposium, Perth, March 1991. J. R. Soc. West. Aust. 74, 101–114.

Marba, N., Duarte, C.M., 2010. Mediterranean warming triggers seagrass (*Posidonia oceanica*) shoot mortality. Glob. Change Biol. 16, 2366–2375 http://dx.doi.org/10.1111/j.1365-2486.2009.02130.x.

Maxwell, J.G.H., Cresswell, G.R., 1981. Dispersal of tropical marine fauna to the Great Australian Bight by the Leeuwin Current. Aust. J. Mar. Freshwat. Res. 32, 493–500.

Micha, A., 2011. Some new visitors to the Busselton Underwater Observatory. In: Pearce, A.F., Lenanton, R., Jackson, G., Moore, J., Feng, M., Gaughan, D. (Eds.), The 'Marine Heat Wave' Off Western Australia during the Summer of 2010/2011. : Dept. Fish. West. Aust. Res. Rept., 222. Department of Fisheries, Western Australia, pp. 14–15.

Moore, J., Bellchambers, L., Depczynski, M., Evans, R., Evans, S., Field, S., Friedman, K, Gilmour, J., Holmes, T., Middlebrook, R., Radford, B., Ridgway, T., Shedrawi, G., Taylor, H., Thomson, D., Wilson, S., submitted for publication. Anomalous ocean warming and cyclonic activity in 2010–11 drive unprecedented regional-scale bleaching and loss across Western Australian coral reefs. Plos One.

Munday, P.L., Jones, G.P., Sheaves, M., Williams, A.J., Goby, G., 2007. Vulnerability of fishes to climate change: exposure and sensitivity. In: Johnson, J.E., Marshall, P.A. (Eds.), Climate Change and the Great Barrier Reef. Great Barrier Reef Marine Park Authority and Australian Greenhouse Office, pp. 357–391.

Neuheimer, A.B., Thresher, R.E., Lyle, J.M., Semmens, J.M., 2011. Tolerance limit for fish growth exceeded by warming waters. Nature Clim. Change 1, 110–113.

Olita, A., Sorgente, R., Natale, S., Gaberšek, S., Ribotti, A., Bonanno, A., Patti, B., 2007. Effects of the 2003 European heatwave on the Central Mediterranean Sea: surface fluxes and the dynamical response. Ocean Sci. 3, 273–289 http://dx.doi.org/10.5194/os-3-273-2007.

Oliver, E.C.J., Thompson, K.R., 2011. Sea level and circulation variability of the Gulf of Carpentaria: influence of the Madden–Julian Oscillation and the adjacent deep ocean. J. Geophys. Res. 116, C02019 http://dx.doi.org/10.1029/2010JC006596.

Pearce, A.F., 1991. Eastern boundary currents of the Southern Hemisphere. J. R. Soc. West. Aust. 74, 35–45.

Pearce, A.F., Feng, M., 2007. Observations of warming on the Western Australian continental shelf. Mar. Freshw. Res. 58, 914–920.

Pearce, A.F., Hutchins, J.B., 2009. Oceanic processes and the recruitment of tropical fish at Rottnest Island (Western Australia). J. R. Soc. West. Aust. 92, 179–195.

Pearce, A., Lenanton, R., Jackson, G., Moore, J., Feng, M., Gaughan, D., 2011. The "Marine Heat Wave" Off Western Australia during the Summer of 2010/11. : Dept. Fish. West. Aust. Res. Rept., 222. Department of Fisheries, Western Australia (36 pp.).

Pearce, A.F., Lynch, M.J., Hanson, C.E., 2006. The Hillarys transect (1): seasonal and cross-shelf variability of physical and chemical water properties off Perth, Western Australia, 1996–98. Cont. Shelf Res. 26, 1689–1729.

Pearce, A.F., Phillips, B.F., 1988. ENSO events, the Leeuwin Current, and larval recruitment of the western rock lobster. ICES J. Mar. Sci. 45, 13–21.

Perry, A.L., Low, P.J., Ellis, J.R., Reynolds, J.D., 2005. Climate change and distribution shifts in marine fishes. Science 308, 1912–1915.

Reynolds, R.W., Smith, T.M., 1994. Improved global sea surface temperature analyses using optimal interpolation. J. Clim. 7, 929–948.

Sandery, P., 2011. Significant mesoscale oceanography: summer 2010/2011. Bull. Aust. Met. Oceanogr. Soc. 24, 48–49.

Schar, C., Vidale, P.L., Luthi, D., Frei, C., Haberli, C., Liniger, M.A., Appenzeller, C., 2004. The role of increasing temperature variability in European summer heatwaves. Nature 427, 332–336.

Smale, D.A., Wernberg, T., 2009. Satellite-derived SST data as a proxy for water temperature in nearshore benthic ecology. Mar. Ecol. Prog. Ser. 387, 27–37.

Smale, D.A., Wernberg, T., 2012. Ecological observations associated with an anomalous warming event at the Houtman Abrolhos Islands, Western Australia. Coral Reefs 31, 441 http://dx.doi.org/10.1007/s00338-012-0873-4.

Smith, K.A., Chambers, N., Jackson, G., 2011. Unusual biological events coinciding with warm ocean conditions along the south-west coast of WA. In: Pearce, A.F., Lenanton, R., Jackson, G., Moore, J., Feng, M., Gaughan, D. (Eds.), The 'Marine Heat Wave' Off Western Australia during the Summer of 2010/2011. : Dept. Fish. West. Aust. Res. Rept., 222. Department of Fisheries, Western Australia, p. 11.

Smith, K.A., Hammond, M., Close, P.G., 2010. Aggregation and stranding of elongate sunfish (*Ranzania laevis*) (Pisces: Molidae) (Pennant, 1776) on the southern coast of Western Australia. J. R. Soc. West. Aust. 93, 181–188.

Smith, R.L., Huyer, A., Godfrey, J.S., Church, J.A., 1991. The Leeuwin Current off Western Australia, 1986–87. J. Phys. Oceanogr. 21, 323–345.

Sparnocchia, S., Schiano, M.E., Picco, P., Bozzano, R., Cappelletti, A., 2006. The anomalous warming of summer 2003 in the surface layer of the Central Ligurian Sea (Western Mediterranean). Ann. Geophys. 24, 443–452 (http://www.ann-geophys.net/24/443/2006/).

Speed, C.W., Meekan, M.G., Russell, B.C., Bradshaw, C.J.A., 2009. Recent whale shark (*Rhincodon typus*) beach strandings in Australia. Mar. Biodivers. Rec. 2, 1–3 http://dx.doi.org/10.1017/S1755267208000158.

Sporer, E., Kangas, M., 2011. Prawn recruitment trends and scallop growth in Shark Bay during 2010/2011 — observations after unusually warm sea temperatures and flood events. 2011 In: Pearce, A.F., Lenanton, R., Jackson, G., Moore, J., Feng, M., Gaughan, D. (Eds.), The 'Marine Heat Wave' Off Western Australia during the Summer of 2010/2011. : Dept. Fish. West. Aust. Res. Rept., 222. Department of Fisheries, Western Australia, p. 12.

Sutton, R.T., Hodson, D.L.R., 2004. Atlantic ocean forcing of North American and European summer climate. Science 309, 115–118.

Sylvester, J.R., 1972. Possible effects of thermal effluents on fish: a review. Environ. Pollut. 3, 205–215.

Taylor, J.G., 1994. Whale Sharks, the Giants of Ningaloo Reef. Angus and Robertson, Sydney. (176 pp.).

Thomson, D.P., Bearham, D., Graham, F., 2011. High latitude, deeper water coral bleaching at Rottnest Island, Western Australia. Coral Reefs http://dx.doi.org/10.1007/s00338-011-0811-x.

Wernberg, T., Smale, D.A., Tuya, F., Thomsen, M.S., Langlois, T.J., de Bettognies, T., Bennett, S., Rousseaux, C.S., 2012. An extreme climatic event alters marine ecosystem structure in a global biodiversity hotspot. Nature Clim. Change http://dx.doi.org/10.1038/nclimate1627.

Wilson, B.R., Allen, G.R., 1987. 3. Major components and distribution of marine fauna. In: Dyne, G.R., Walton, D.W. (Eds.), Fauna of Australia, vol. 1A. Aust. Gov. Publ. Serv, Canberra, pp. 43–68.

Wilson, S.G., Polovina, J.J., Stewart, B.S., Meekan, M.G., 2006. Movements of Whale Sharks (*Rhincodon typus*) tagged at Ningaloo Reef, Western Australia. Mar. Biol. 148, 1157–1166.

Wilson, S.G., Taylor, J.G., Pearce, A.F., 2001. The seasonal migration of whale sharks at Ningaloo Reef, Western Australia: currents, seasonal migrations and the El Nino/Southern Oscillation. Environ. Biol. Fishes 61, 1–11.

Wolter, K., Timlin, M.S., 1998. Measuring the strength of ENSO events — how does 1997/98 rank? Weather 53, 315–324.

Woo, M., Pattiaratchi, C.B., 2008. Hydrography and water masses off the Western Australian coast. Deep Sea Res. I 55, 1090–1104.